PSEUDOKARST TOPOGRAPHY IN A HUMID ENVIRONMENT CAUSED BY CONTAMINANT-INDUCED COLLOIDAL DISPERSION

A Thesis

by

DOUGLAS SPENCER SASSEN

Submitted to the Office of Graduate Studies of
Texas A&M University
in partial fulfillment of the requirements for the degree of

MASTER OF SCIENCE

December 2003

Major Subject: Geology

PSEUDOKARST TOPOGRAPHY IN A HUMID ENVIRONMENT CAUSED BY CONTAMINANT-INDUCED COLLOIDAL DISPERSION

A Thesis

by

DOUGLAS SPENCER SASSEN

Submitted to the Office of Graduate Studies of
Texas A&M University
in partial fulfillment of the requirements for the degree of

MASTER OF SCIENCE

Approved as to style and content by:

Christopher C. Mathewson (Chair of Committee)	Mark Everett (Member)
Jean-Louis Briaud (Member)	Richard Carlson (Head of Department)

December 2003

Major Subject: Geology

ABSTRACT

Pseudokarst Topography in a Humid Environment Caused by Contaminant-Induced Colloidal Dispersion. (December 2003)

Douglas Spencer Sassen, B.S., The University of Texas at Austin

Chair of Advisory Committee: Dr. Christopher C. Mathewson

Over fifty small sinkholes (~1 meter in depth and width) were found in conjunction with structural damage to homes in an area south of Cleveland, TX. The local geology lacks carbonate and evaporite deposits associated with normal sinkhole development through dissolution. The morphology and distribution of sinkholes, and the geologic setting of the site are consistent with piping erosion. However, the site lacked the significant hydraulic gradient or exit points for sediment associated with traditional piping erosion. In areas of sinkholes, geophysical measurements of apparent electrical conductivity delineated anomalously high conductivity levels that are interpreted as a brine release from a nearby oil-field waste injection well. The contaminated areas have sodium adsorption ratios (SAR) as high as 19, compared to background levels of 3. Sodium has been shown to cause dispersion of soil colloids, allowing for sediment transport at very low velocities. Thus, subsurface erosion of dispersed sediment could be possible without significant hydraulic gradients. This hypothesis is backed by the observation of the depletion of colloidal particles within the E-horizon of sinkholes. However, there is a lack of precedence of waste brines initiating colloid dispersion.

Also, sodium dispersion is not thought to be an important process in piping erosion in humid settings such as this one. Therefore, laboratory experiments on samples from the site area, designed to simulate field conditions, were conducted to measure dispersion verses pH, SAR and electrical conductivity (EC). Analysis of the experimental data with neural networks showed that an increase in SAR did increase dispersion. A dispersion prediction map, constructed with the trained neural network and calibrated geophysical data, showed correlation between sinkhole locations and increased predicted dispersion. This research indicates that a contaminant high in sodium content has caused colloidal dispersion, which may have allowed nontraditional subsurface erosion to occur in an area lacking a significant hydraulic gradient.

ACKNOWLEDGMENTS

I thank the many people who helped me with this work. I thank the Aldredge Family for use of their land in the investigation of this problem. Faculty and staff from several departments donated their time and resources to help with this research. From the Department of Soil and Crop Sciences I thank Dr. Charles Hallmark for the use of the Soil Characterization Laboratory. Donna Prochaska, the laboratory analyst for the Soil Characterization Laboratory, gave much of her time and effort into training me on techniques of soil characterization. From the Department of Civil Engineering, I thank Mike Linger for the use of the Geotechnical Laboratory for grain size analysis and for his advise on life. From the Department of Geology and Geophysics, I also thank Bruce Herbert and Ray Guillemette for their help and encouragement in perusing the theory of colloidal dispersion. Jim Carter, Samir Chandra, and Carl Pierce gave up their weekends and sometimes blood while helping me with site work in the mosquito infested fields of Cleveland, Texas. Of course, I thank my committee members for their thoughts and input into this thesis. Dr. Mathewson has been the key mentor in my life for the last 2 years. Foremost, I thank my wife. Thank you for your understanding while I worked through many weekends and late nights.

TABLE OF CONTENTS

Page

CHAPTER Page

LIST OF FIGURES

FIGURE Page

LIST OF TABLES

CHAPTER I

INTRODUCTION

In the spring of 2001, a homeowner contacted the Geology and Geophysics Department with regard to the unexplained appearance of holes in the backyard and structural damage to the home. Initial inspection of the site confirmed the homeowner's claims. Some holes where 1.5 meters deep and 2 meters wide. The house showed many signs of differential settling, including cracked dry wall and mortar, leaking roof, and jammed doors and windows. According to the owners, the house was built over thirty years ago. The landowners placed the initial timing of the damage to coincide with the initial appearance of the sinkholes, about 7 to 8 years previous and more than 26 years after construction. The timing of the damage does not fit with normal settlement processes. It was hypothesized that the same process that created the sinkholes caused the damage. The apparent sinkholes seem to form a channel-like pattern, as one would expect from piping erosion. However, the normal paradigm for piping erosion includes steep slopes and outlets found in embankments (Higgins, 1984, and Parker et al., 1990) neither of which was found. The origin of the sinkholes was decided to be of unknown cause. The research herein is directed to find the processes behind the sinkholes in hopes that an efficient and effective method of fixing the problem is found, and to provide a guide for future workers encountering similar issues.

This thesis follows the format and style of *Environmental and Engineering Geoscience.*

Setting

The site is located approximately 2 miles south of Cleveland, Texas and approximately 43 miles northeast of Houston, TX. The surficial geology of the area is clastic sediments of the Lissie Formation. This formation parallels the current coast of the Gulf of Mexico from western-coastal Louisiana to central-coastal Texas. It has been dated to approximately 0.75 Ma, the early Pleistocene (Bowen, 1978) and interpreted as an abandoned alluvial deltaic plain (Benard et al., 1962). The topography is slightly rolling, incised rivers and creeks account for the variation in elevation. The relief of this region is 40 feet [12.3 meters] with a maximum elevation of 150 feet [46 meters]. The gradient of the site is nearly horizontal with a slight slope from the south to the north. The natural vegetation in the area consists of pine, deciduous trees, and thick undercover. The soil at this site is of the Ultisol and Alfisol orders (Freed et al., 1996). The site lacks any carbonate or evaporite deposits needed for classic sinkhole development.

Guiding Principle

On geologically short time spans (100's to 1000's of years) landscapes are usually in steady-state equilibrium with their environment (Bloom, 1998). In this state, change to the landscape usually consists of small perturbations around some average state. The landscape will continue in this state until some external change in the environmental system causes the landscape to respond and change to a new metastable equilibrium. Sudden changes in the landscape may be attributed to a sudden change in

the environment. Plus, change in the landscape may not occur instantaneously, pressures on the landscape may build until a threshold is reached and there is then a sudden response. The development of sinkholes in a very short time span in an area where they are otherwise unheard of, indicates that the landscape or subsurface is somehow out of equilibrium with its environment. The question becomes is this change a response to environmental pressures that have been building for some time, or has some recent change in the environment incited the development of these sinkholes?

One approach to study this problem is to look for geomorphic indicators of the state of a landscape. One of the most useful geomorphic indicators is soil development. It takes considerable time to develop definable soil horizons on a newly formed landscape. Even in humid regions with easily weathered material and intense biologic activity, 2,000-3,000 years are necessary to show significant profile development (Foss and Segovia, 1984). Strong soil horizons will not form if the site is being actively eroded or has active deposition. The soils at the study site is of the Ultisol and Alfisol orders (Freed et al., 1996). These soils are highly weathered, have very strong soil horizons, and plinthite (oxide concretions). This indicates a very mature soil that took considerable time to form under nearly steady state conditions. A minimum time span of thousands of years should be sufficient for a landscape such as the study site to reach steady state equilibrium.

The climate and topography of the area has also been relatively constant over the last 6,000 years. The underlying geology, the Lissie formation, is a recent depositional feature that has not changed much in 0.75 million years since its formation. The

topography is very subdued, with very gentle gradients. It could be argued that the last major influence to the area's geomorphology is from the end of the last ice age 18,000 years ago, which led to a rapidly changing climate. However, climatologists believe that the current climate reached equilibrium approximately 6,000 years ago and has changed little since (Williams et al., 1998). The local climate is not restricted by topography and is dominated by latitude and oceanic influences. Aside from short-term climatic variations, the study site has had sufficient time to respond to the current climate and topography.

From this evidence, it seems more likely that the sinkhole development is from a short-term change in the environment, most probably induced by anthropogenic activity. From this guiding principle the initial investigation into the cause of the sinkholes focuses on the factors that would change the landscape's topography, biologic activity, hydrology, soil mechanics, and chemistry in the very short term.

Recent Environmental Changes

General observations and interviews with local residents were carried out to identify factors that could place environmental pressures on the site. During the interviews with homeowners, several interesting claims and facts about the history of the site and surrounding areas came to light. The first interesting claim is the burial of stumps and logs in deep pits on the site. An interview with Mr. Tomayo revealed that the original owner and developer in the study area had dug pits in which logs and stumps were buried. Tomayo never saw this in first-person, he obtained this information from

his father. The timing of the burial of tree debris is unclear, but the best guess is 30 years ago. Decay or compression of decay matter can lead to the development of sinkholes. Another fact of interest is the existence of a wastewater injection well near the site. This well, and associated storage tanks, is approximately 10 meters south of the access property line. Charles Aldredge said that the well is used for injection of brine wastewater deep into the ground. He has witnessed several problems with the well, including surface spills and the replacing of the well pipe. Charles Aldredge also observed that the clearing of a nearby field coincided with the appearance of the sinkholes. The field south of the Aldridge property had been cleared 9 years ago, just prior to the development of the first holes (Figure 1). The removal of the trees could disrupt the normal equilibrium of the water table level and soil chemistry by lowering the relative level of evapotransportation and increasing runoff.

(The star is located over the study site)

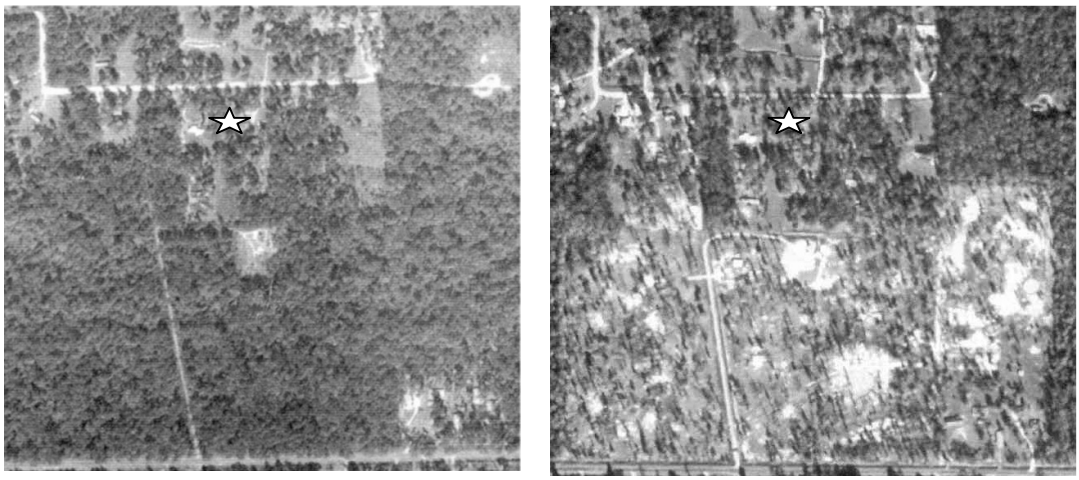

1988 ***1996***

Figure 1. Aerial photographs of study area before and after land clearing.

Another possibly pertinent observation is the abundance of oil-field wells in the area. Oil-field production could contribute to land subsidence. From these potential environmental pressures and the general morphology of the sinkholes, several hypotheses were formulated that could explain the timing and distribution of these sinkholes.

Assessment of Multiple Hypotheses

Given the setting and history of the site, several working hypotheses arose to explain the development of the sinkholes. Literature reviews of similar occurrences revealed three main processes that can lead to the observed sinkholes in this geologic setting. These processes are earth fissuring, material dissolution, and piping erosion. One or any combination of these general processes could result in sinkholes.

Earth Fissures

Earth fissures are steep-sided crevasses at the surface that are related to tensional forces from differential subsidence, which is strongest on boundaries where the bedrock depth changes from shallow depths to great depths (Holtzer, 1984). Subsidence will be greater in areas in which there exists thicker sequences of unconsolidated material, and less in the areas in which the bedrock is close to the surface and thus the unconsolidated thickness is less (Holtzer, 1984). These fissures are often linear in shape and large in size, 100 to1000's of meters in length (Pewe, 1990).

The subsidence is caused by removal of pore pressure by overproduction of subsurface fluids or natural dewatering. Water pumping, and oil-field and gas production are common sources for removal of pore pressure. The reduced pore pressure allows consolidation of sediment grains into a smaller volume. It also increases the effective stress on the sediments as a whole.

The regional area of the site has thick sequences of unconsolidated material high in pore fluids. The area has been intensively developed for oil and gas throughout the century and also for municipal wells to produce water. The oil and gas production has centered on salt domes. These salt domes could provide the consolidation material needed for differential subsidence. If this process is in part to blame, the sinkholes should make a relatively linear pattern parallel to known salt dome margins and extend well beyond the area of the site. Looking at a plot of the locations of each sinkhole, the overall pattern is not strongly linear or large scale (Figure 2).

Material Dissolution and Decay

If the reported buried wood does, in fact, exist it could provide a source for sinkhole development. The wood could have experienced rapid decay following a change in the shallow groundwater levels. This decay would open void space into which soil could collapse. Although burial pits have not been found, if this were the case the sinkholes should have a clustering around burial sites. As seen in Figure 2, this is not the case. However, the void space from decaying organic matter could provide a sink for sediment in other processes such as piping erosion.

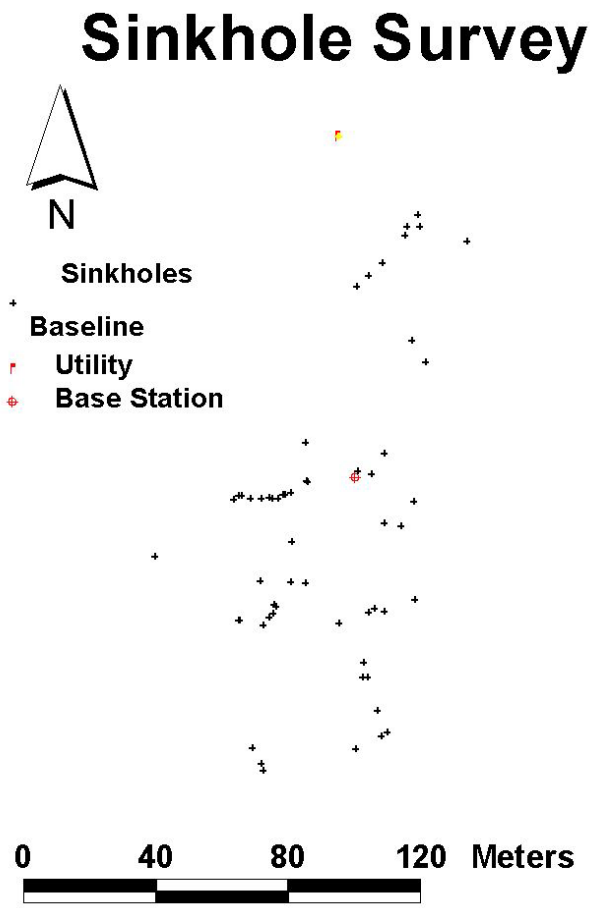

Figure 2. Survey of sinkhole locations.

Another possible explanation came up during literature review, the possibility of volume loss caused by mineral dissolution and or alteration. Isphording and Flowers (1988) published a paper on the formation of small sinkholes caused by the alteration of kaolinite to gibbsite (Figure 3). Their research focused on a site with very similar soil and climatic conditions. There is a 35% reduction in volume from the transformation of kaolinite to gibbsite (Isphording and Flowers, 1988).

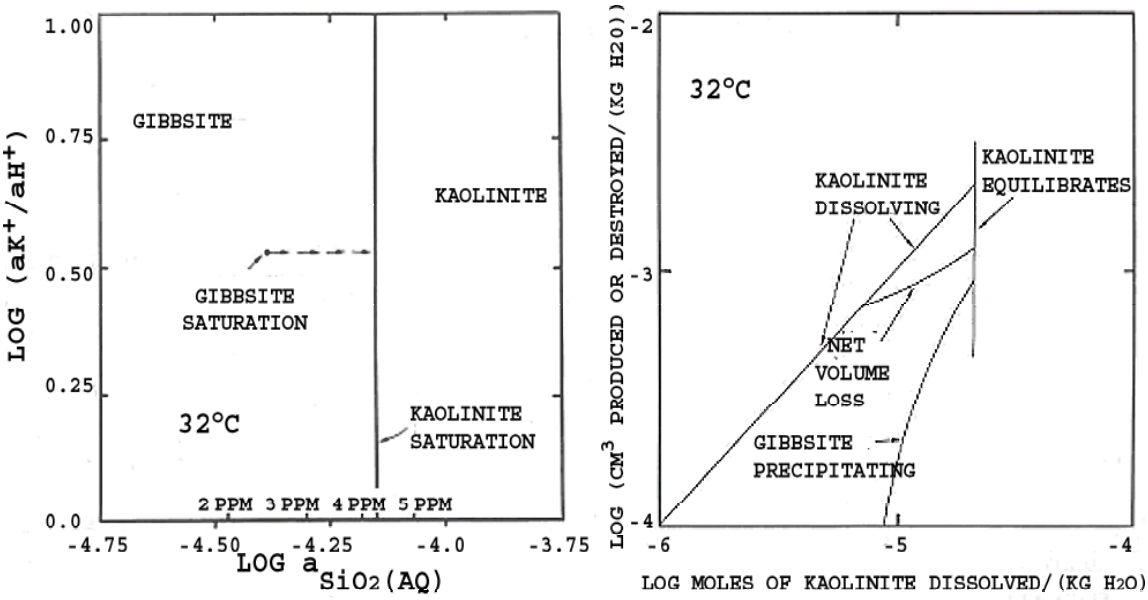

Figure 3. Stability of kaolinite and gibbsite (Isphording and Flowers, 1988).

The basis of this idea is that kaolinite is out of equilibrium with its environment, and that gibbsite is more stable in the conditions of humid climates. Their assessment came under criticism by Dal Hunter and others (1989), who pointed out that the volume loss was impossible with the conditions held by Isphording and Flowers. The clay content of the soil was only 10% and a total replacement in kaolinite with gibbsite would result in 35% reduction in volume of that 10% or 3.5% of the soil (Hunter et al., 1989). Also, the kinetics of this reaction was not considered. Minerals may remain in a state of non-equilibrium for some time before altering to a more stable mineral. Kaolinite is one of the slowest weathering minerals in natural soil, it takes 6 million years to weather a 1mm cube of kaolinite at a pH of 5 and a temperature of 25°C (Langmuir, 1997). It is highly unlikely that the alteration of kaolinite to gibbsite will lead to sinkhole development in a very short period of time.

Hunter and others (1989) put forth an alternate hypothesis for the sinkholes of Isphording and Flowers that placed the probable mechanism on the dissolution of iron hydrous-oxide cements from reaction with acidic groundwater. A shift in the geochemical state of the groundwater and soil could cause dissolution of iron hydrous-oxides that may act as cements in the soil. Clearing of the land could provide this shift by changing the evapotranspiration and infiltration rates thus affecting the mean water table level and redox state. Dissolution of these cements could lead to only a small loss of volume, but could decrease cohesion in the soil. However, this hypothesis alone would not explain why the sinkholes are only restricted to a small portion of the land. A change in the shallow water table and thus geochemistry would affect a larger area than the observed extent of the sinkholes.

Piping Erosion

The final and most promising hypothesis, piping erosion, would produce a sinkhole morphology and distribution much like what is seen at the study site. There are several characteristics conducive to piping erosion. These characteristics include: an initial opening or macropores, hydraulic gradient to attain water velocities sufficient for sediment entrainment, erodible sediment, and a sink or output for the transported sediment (Higgins and Schoner, 1997, Higgins 1984).

Inflow sites are needed for the rapid infiltration of water into the unsaturated subsurface. In most studies, these inflow sites are provided by desiccation cracks. Animal burrows, rotted roots, anthropogenic disturbances may also provide for inflow

sites (Cedergren, 1977). At the Aldredge site the most probable source of the inflow sites would be animal burrows and rotting organic material. Gophers and crawfish are prolific in the area. The fine-sand and silt content of the soil is too high for desiccation cracks to form. Substantial infiltration of runoff is needed to provide the volume and velocity of water to entrain sediments in the subsurface. During extremely intense rains, runoff will occur even before the soil has become saturated providing optimal conditions for subsurface erosion. At the study site very intense afternoon thunderstorms are a common occurrence during the warmer half of the year. Once initial opening and void spaces are provided these spaces must be enlarged. Water flowing through these openings can entrain the sediments if the sediment is unconsolidated and the velocities are sufficient. However, the sediment must be cohesive enough to maintain the structure of the tunnels (Higgins, 1984). Also, water velocity and turbulence is usually only enough to entrain very fine sediments such as fine sand or silts. Most of the literature concerning sediment requirements focuses on soil with high amounts of dispersible clays. The dispersion of the clay allows for the entrainment of normally consolidated sediment. The proportions of silt to clay, the expansive properties of clays and dispersing agents have all been studied extensively by previous authors. It has been found that the addition of salts, especially Na^+ ions, can cause dispersion in clays that are not particularly expansive (Faulkner et al., 2000, Minhas et al., 1999). The brine injection well and its associated problems could provide a source of sodium for dispersion. Also, the previously mentioned possibility of the dissolution of iron hydrous-oxides could allow entrainment of normally stable soil.

The final requirement for piping erosion is the output or sink of the entrained sediment. Most commonly the sediment output is an outlet of the pipe in an embankment or stream channel. This is most commonly the case in hilly areas. Sinks, such as void space created by mineral dissolution, organic decay or compaction are other possibilities. Higgens and Schoner (1997) researched sinkholes formed by the piping into buried channels. They described the process of eluviation as the process by which fine-grained materials such as silt or clay are transported to the large voids found in well-sorted coarse deposits (Parker et al., 1990). Because the depositional history of the underling geology at the study site is fluvial, there is the possibility that coarse-channel gravel and sand could be in the shallow subsurface providing a sink for finer grained material.

Piping erosion is the most promising theory for the development of the sinkholes at the study site for several reasons. The presence of piping erosions may be an indicator that a landscape is unstable and changing (Berger and Aghassy, 1984). The consequences of the clearing of the land, presence of a wood burial pit, and possible brine contamination could each cause or contribute to the process of piping erosion. Thus, it would fit with the guiding principle and timing of these sinkholes. Also, unlike other hypotheses put forth, the sinkholes' size and distribution is similar to previous cases of piping erosion. However, several conditions for piping erosion are not yet apparent at the site, nor is the environmental change that may have lead to piping.

Research Objectives

The objective of my research is to find the cause of the sinkholes through geologic, geochemical and geophysical methods. The hope is that by finding the cause of the problems a corrective measure can be formulated that efficiently and inexpensively restores the site to an acceptable state. This will also act as a case study for other practitioners who encounter similar problems. The hypothesis that piping erosion is the cause of the sinkholes is stronger than the others on the grounds of the distribution of the sinkholes as well as the characteristics of the site that could contribute to this process. The anthropogenic influences on the environment of the site could contribute to the initiation of piping. Therefore, the research focus is on determination of what external influences caused the piping.

CHAPTER II

SITE INVESTIGATION

Introduction

A preliminary study of the site included personal interviews, historical photographic analysis, literature review, visual inspections, and a survey of sinkhole locations. From this initial study, the most likely cause of the sinkholes at the site is thought to be piping erosion. This preliminary study failed to find an outlet or sink for the pipes, or to find the factor that initiated this process. Also, the question of why these sinkholes have appeared in this localized area in a very sudden time period is unresolved. There is a substantial list of possible events and site properties to which the piping and sinkhole development could be attributed. Thus, the investigation needs to be analytical and efficient.

In a situation like this, where little is known of the processes behind the problem, there are multiple hypotheses needing large amounts of data for support or dismissal. Funding, resources and time are very limited at the same time. Most geologic subsurface investigations require the drilling of boreholes to properly characterize the subsurface. Lateral surveys of soil also require a substantial amount of samples for proper coverage. Because of cost and time concerns, a drilling or sampling grid with wide spacing is the norm. However, a drilling or sampling grid of this kind can miss important features such as a burn pit, a pipeline, or anomalous mineralogy or chemistry of soil. The conventional wisdom for solving this problem is to tighten the grid spacing.

A more intelligent method would involve the use of rapidly acquired inexpensive data to guide sampling to only the areas of interest.

Geophysical methods can rapidly acquire large amounts of observational data with relatively little cost or disturbance to the site. Therefore, near-surface geophysical techniques were selected as a preliminary subsurface investigation technique for the characterization of the sinkhole development. There are many different geophysical methods available, only those that will yield the most pertinent responses should be utilized. In this case, differences in subsurface texture, mineralogy, water content and aqueous chemistry could all be important factors in the process behind the development of the sinkholes observed at the site. Geophysical methods were selected that would be sensitive to these properties. These include ground penetrating radar (GPR) and frequency domain electromagnetic induction (EM).

The geophysical data guide coring and hydrologic investigations. There are several characteristics of soil that are found to be conducive to piping erosion. These include: a roof material cohesive enough to maintain pipes, and a soil that is easily eroded, naturally dispersive, or a dispersing agent. Piping erosion is a hydrogeologic process that has specific conditions for this process to occur. There are various hydrologic characteristics that are conducive for piping erosion. These characteristics include: gradients sufficient for the entrainment and transport of sediment by subsurface flow, a relatively high hydraulic conductivity horizon underlain by a low conductivity layer, and a discharge point or subsurface reservoir for entrained sediment. Along with geophysical methods, coring and hydraulic testing can provide the samples needed to

investigate the subsurface parameters that may be conducive to piping. This study will utilize these three investigation techniques to studying the apparent piping erosion at this site. The overall goal of which is to determine what environmental change has initiated the appearance of piping and associated sinkholes.

Methods and Results

Frequency domain electromagnetic survey techniques are based on the induction of current loops in the subsurface. A transmitter sends a current through a loop that in turn induces a current loop in the conductive he subsurface, which in turn induces a current in a receiving coil. The current induced in the receiver is dependent upon the intensity, orientation and position of the induced current in the ground (Sharma, 1997). The subsurface current is dependent on how the subsurface conducts electricity, which is dependent on mineralology, texture, pore fluid composition and saturation of the subsurface (Everett, 2002). In the study of the sinkholes, all of these properties are of interest. Thus, the electromagnetic method provides an indirect method to study the site characteristics that may lead to sinkhole development. Data gained from the electromagnetic survey can be used to guide direct sampling that can validate interpretations.

There are several considerations in the depth and area of response used in designing a survey for specific problems. Frequency-domain electromagnetics provides a bulk measurement of the near surface; most of the response comes from the area of peak induced current flow. The depth from which the bulk of the response comes from

is usually less than 1.5 times the transmitter and receiver separation (McNeill, 1980). In this case the response depth is limited to approximately 6 meters.

Electromagnetics Survey Design

For the first survey, the lateral electrical conductivity of the study site was measured using frequency-domain electromagnetics. The survey was designed to efficiently cover the study site and to correlate certain responses with the sinkhole appearance. The electrical conductivity was measured using a Geonics EM-31 terrain conductivity meter. The survey was a 2-dimensional grid, based on the benchmark used from the survey of the sinkhole locations. The grid size was determined based the spatial resolution of the instrument and time considerations. The grid spacing is 15ft (4.6m), and runs north-south and east-west. Measuring tapes stretched between control points, that were surveyed using a theodolite and a stadia rod, controlled the position of each measurement. At each grid point a reading of the electrical conductivity was taken and recorded. From the data, a conductivity map was constructed in spatial graphing software using the nearest-neighbor interpolation between the known points.

Electromagnetics Results

Figure 4 shows the results of the electrical conductivity survey overlaid with the locations of the sinkholes. There are considerable sources of interference on the field survey area. A large portion of the backyard is used for storage of automobiles, airplanes, cargo containers and various other metal objects.

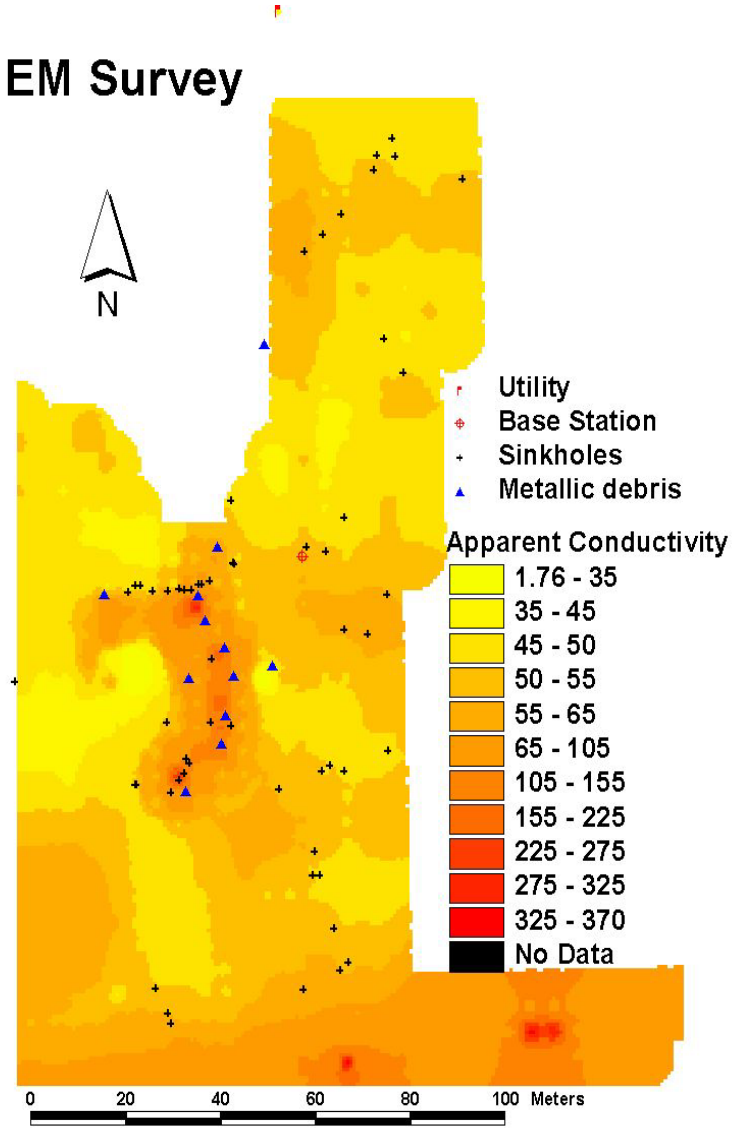

Figure 4. Apparent conductivity (mS/m) measurements of the site.

Because metal is highly conductive it contributes significantly to the total induced current. This contribution cannot be differentiated from the bulk ground response. Areas immediately around these sources of interference were recorded and displayed, but are not considered representative of the apparent ground conductivity. It

was also noticed that readings of conductivity greatly increased toward the southern end of the survey area that approaches the injection well. During interviews it was discovered that this injection well is used for underground disposal of waste oil-field brine, and that the well casing had to be replaced because of leaks. Also, a surface spill was observed and evaporite crystals were seen at the surface. This high conductivity zone is most probably from a surface spill because the trend of the high conductivity areas running parallel to a shallow drainage ditch. In the areas where the interference was not a problem, it was noticed that areas close to sinkholes had slightly higher values of conductivity than areas away from sinkholes. This could indicate that the brine from the injection affected areas of the sinkholes as well. At the same time, no sinkhole is found in the areas of high apparent electrical conductivity. It should be noted that the apparent electrical conductivity of the ground is not solely dependant upon the ion concentration in pore solution. Thus, direct sampling would be needed to conclusively link higher apparent electrical conductivity with increased salt concentrations in the soil.

Ground Penetrating Radar

The second geophysical technique, GPR, was used for generating subsurface profiles. Ground-penetrating radar (GPR) uses electromagnetic waves, which are sensitive to electrical conductivity and dielectric properties of the subsurface material. A GPR unit consists of a radar wave transmitter, a receiver, and a console that records travel time and amplitude of the reflected waves. A transmitted radar wave passing from a material of a given dielectric constant to a material of different dielectric constant will

cause a reflection in all directions including back to a receiving antenna. The total travel time of the recorded reflection is a function or distance from the transmitter to the reflector and back to the receiver multiplied times the velocity of the wave in the subsurface. The velocity of the wave is inversely proportional to the dielectric properties of the subsurface (Table 1). The strength of the reflection will depend on the contrast of the dielectrics from the host media and the target. The strength of reflection also known as the reflection coefficient is described by the following equation:

$$K = \frac{(\sqrt{\varepsilon}_{r2} - \sqrt{\varepsilon}_{r1})}{(\sqrt{\varepsilon_{r2}} + \sqrt{\varepsilon_{r1}})}$$

where K is the strength of the reflection, ε_{r1} is the dielectric of the initial media, and ε_{r2} is the dielectric of the target media (Sharma, 1997). This allows the GPR unit to image changes in pore-water chemistry, saturation, mineralogy, and texture of the subsurface.

Table 1. *Dielectric properties and radar velocities of common earth materials (Sharma, 1997).*

Material	Dielectric Constant	Velocity (m/ns)
Dry sand/gravel	4 to 10	0.15-0.09
Wet sand/gravel	10 to 20	0.09-0.07
Dry clay/silt	3 to 6	0.17-0.12
Wet clay/silt	7 to 40	0.11-0.05
Cement (dry/wet)	6 to 11	0.12-0.09
Granite	4 to 9	0.15-0.10
Limestone	4 to 8	0.15-0.11
Dry salt	5 to 6	0.13-0.12
Permafrost	4 to 5	0.15-0.13
Glacier ice	3.5	0.16
Fresh water	81	0.03
Methyl alcohol	31	0.05
Petroleum/Kerosene	2.1	0.20
Aviation gasoline	1.95	0.21
Air	1	0.30

GPR Survey Design

Several lines of ground penetrating radar data were collected at the site. Using 100MHz antennas, three separate lines of data were collected on various areas of interest. The first acquisition technique was a common mid-point (CMP) gather, which is commonly used in reflection seismology. In the CMP technique the transmitter and receiver are successively moved apart with equal intervals about a common mid-point. This produces a reflection hyperbola off of subsurface reflector surfaces. CMP gathers are useful for finding the velocity of subsurface media, and the depth of layer reflections. The total travel time of the reflected radar wave, and thus the velocity and depth, can be found from the following equation:

$$T = \sqrt{t_o + \frac{X^2}{V^2}}$$

where T is the total travel time of the reflection, t_o is the two way travel time at the common mid-point, X is the distance of the antenna from the common mid point, and V is the velocity of the subsurface media. The second and most commonly used technique for this study was reflection acquisition. This acquisition method is used for the imaging of the subsurface. Both the transmitter and receiver are moved together, with a constant separation, along a survey line to produce a 2-D image of the subsurface. In this case, the lateral spacing between readings was 20cm and the antennas were separated by 1 meter. Like CMP gathers this technique also gives reflection data for continuous surfaces, but is also useful for imaging discontinuous reflectors and point target.

Results and Interpretation of Ground Penetrating Radar

The common mid-point acquisition line is located in the northern end of the site away from the high conductivity zone near the injection well. The CMP time section, shown in Figure 5, shows only one strong subsurface reflector that has a velocity of approximately 0.065m/ns. The depth of this reflector is only 1.4 meters down. A plausible interpretation is that this reflector represents a very shallow water table or a clay rich soil horizon. The direct air-wave seen in the upper part of the section has a velocity of the speed of light, 0.3m/ns.

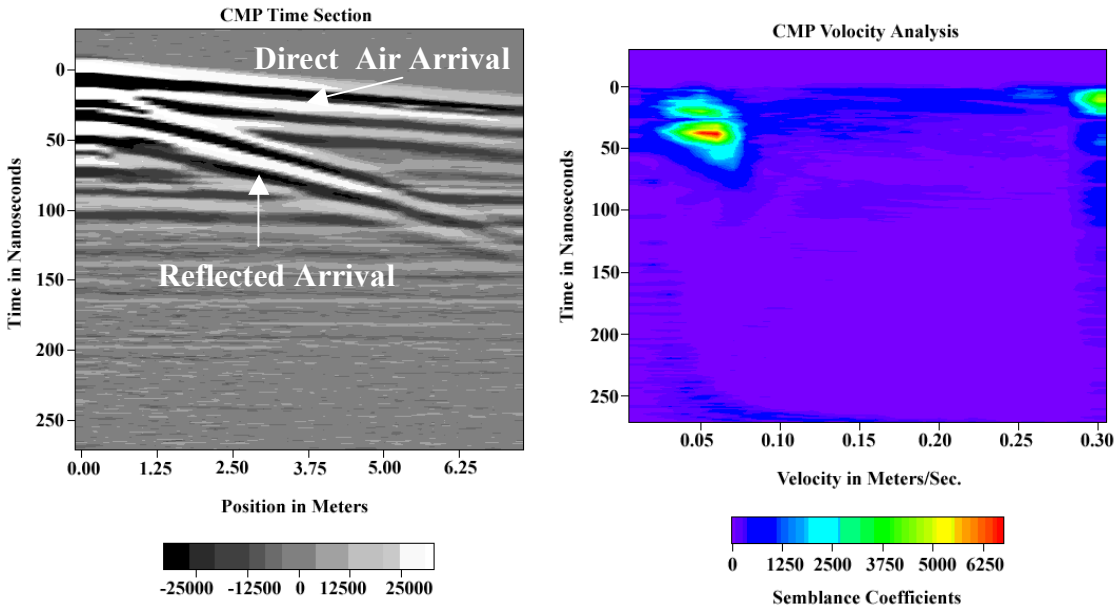

Figure 5. GPR-CMP time section and velocity analysis.

A computer automated CMP velocity analysis is shown in Figure 5. This velocity analysis supports the velocity interpretations from the CMP time section. It also shows

that there are no strong reflections below 60ns or 1.9 meters. This indicates that the signal may be strongly attenuated, or there are no surface reflectors with enough dielectric contrast to produce a reflection.

The first reflection survey was located in area free from sinkholes, trees or surface debris (Figure 6). Because this area was relatively free of sinkholes and noise it is used as a control for comparison of the subsurface response of the sinkhole areas. The coupling of the radar antennas to the ground causes the strong lines seen in the upper meter of the depth section. The coupling zone is not removable through processing and obscures shallow features. Below the coupling zone a reflector surface appears that may correspond to the reflector surface seen in the CMP section. Below that surface are a series of reflectors that were interpreted in the field to be large-scale cross-beds of a fluvial deposit.

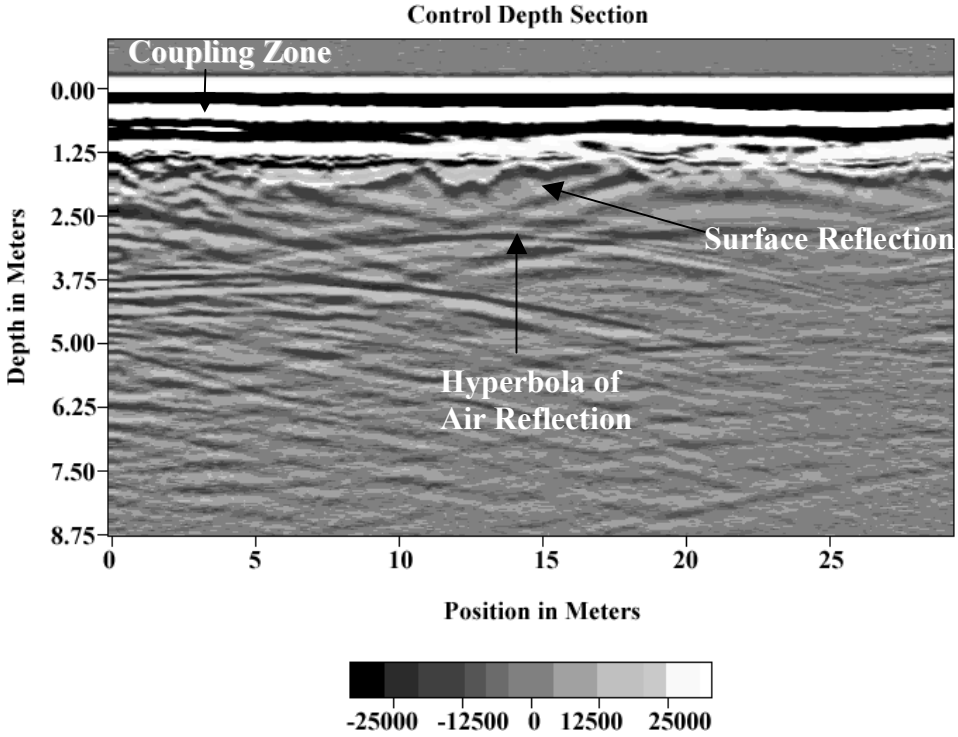

Figure 6. The GPR control depth-section located in an area free of sinkholes.

However, after closer inspection these reflectors are in fact reflected waves from objects above the surface. These features are reflection hyperbolas, whose velocity can be calculated in the same manner as the CMP velocity calculations. Also, the inverse of the slope of the hyperbola, sufficiently far away from its center point, can be used to estimate the velocity of the media through which the reflection traveled. Each of these hyperbolas had an estimated velocity of 0.3m/ns, reflections with velocities this high can only be from travel through air. The source of the air reflectors could be attributed to trees, cars, or small buildings nearby. One can expect to have no useable data from the top meter, and deeper events will be obscured by lack of penetration or air reflectors.

A reflection survey done in an area with sinkholes shows the limitations of this GPR survey. Three strongly dipping diffraction hyperbolas are can be seen in Figure 7. From left to right, the first two hyperbolas seen are interpreted to be from reflections of tree roots directly under the survey line. The last strong hyperbola correlates to point where the survey line passed directly over a sinkhole. This may indicate that a subsurface void exists under the area of the sinkhole, and that it is relatively shallow (1 meter or less).

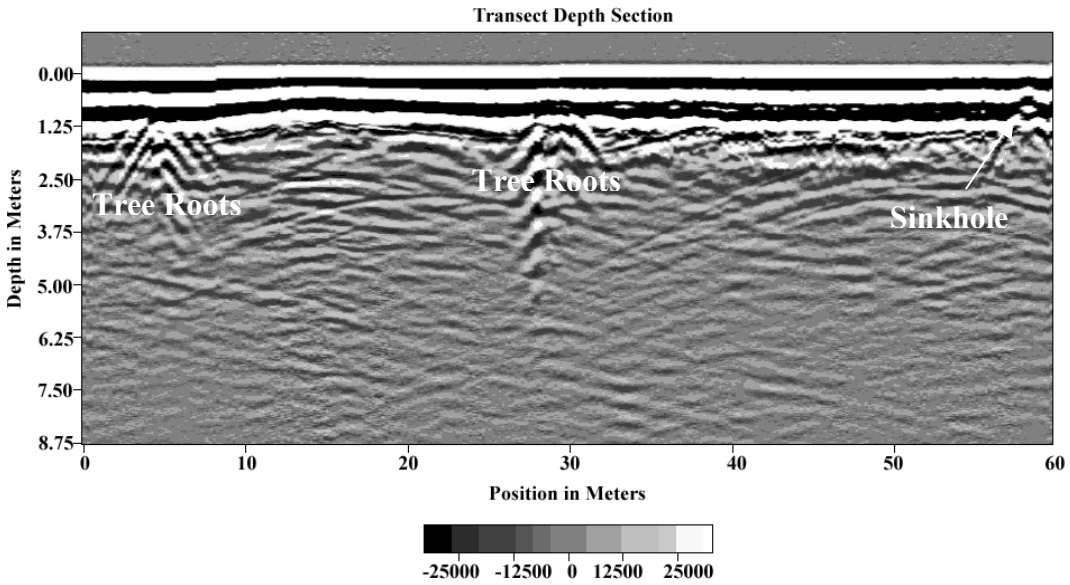

Figure 7. A cross section GPR image of an area of several sinkholes.

If the subsurface features that are leading to the appearance of the sinkholes are in fact this shallow, the GPR configuration will be ineffective at imaging them.

Soil Core Investigation

To describe the shallow subsurface geology of the study site, cores were taken to a depth of approximately 3 meters with a hand auger. Cores were described by texture in the Unified Soil Classification System and by color with the Munsel Soil Color Chart. The soil horizons were defined to show divisions in texture, mineralogy and the soil formation. The Figure 8 shows soil from boreholes 3 and 1.

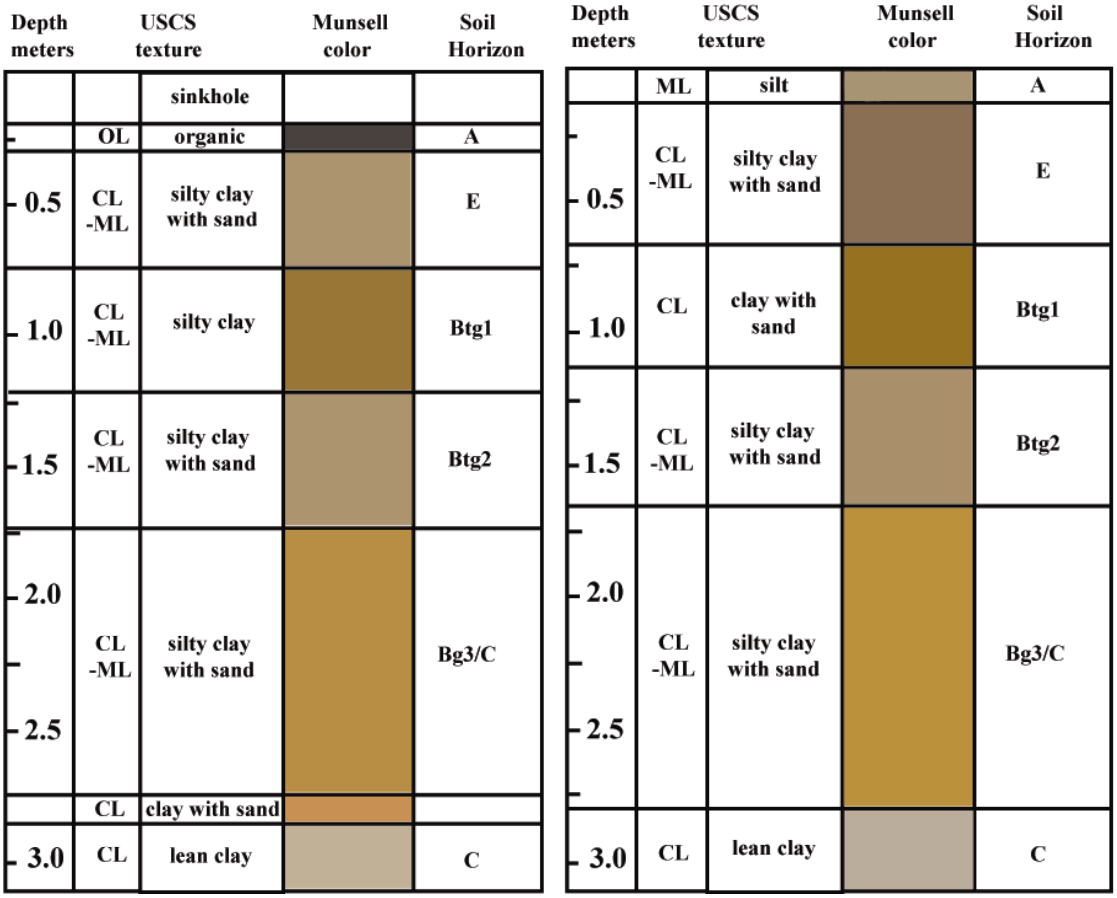

Figure 8. Side by side comparison of cores taken from within a sinkhole (left) and a core taken from outside the sinkhole 1 meter to the west (right).

The cores showed little variation in the soil from one core to the next. The lone exception is borehole 2, which hit buried wood at 0.7 meters down in the area of the presumed disposal pit. The soil ranged in texture from low plastic clay (CL) to low plastic silt (ML). Soils with a CL-ML texture are considered to have almost no cohesion (Das, 2000). During the drilling of boreholes during wetter conditions the E horizon, classified as CL-ML, flowed as a highly viscous fluid into the open borehole. This horizon was saturated and had little cohesion compared to the other horizons in the cores. During dry months the E horizon would be more cohesive because of lower pore pressure, but would be easily eroded when wetted because of its low cohesion. Also, shallow root systems provide a relatively cohesive layer on top of the E horizon. Thus, this horizon is a strong candidate for piping erosion.

In a side-by-side comparison of cores, one core taken in a sinkhole and another taken just a meter away, the horizon with the greatest extent of missing thickness is the E horizon. Also, the E-horizon within the sinkhole is a lighter color than its counterpart. Hydrometer grain size analysis of several depth intervals common between these two cores shows that, within 3 out of the 4 intervals, the grain size distribution varies by only 2-4% by size class (Table 2). However, the depth interval between 61 and 92 cm varies substantially. This interval has a 75% reduction in colloid size particles (<2 microns). Assuming that initially this depth interval was nearly the same between the two cores, then the missing colloid portion would represent a 13% reduction in the soil mass.

Table 2. *Grain size analysis of the cores from Figure 8.*

Core of Sinkhole Borehole 3			**Core 1 Meter from Sinkhole Borehole 1**		
	15 to 35 cm			**15 to 25 cm**	
% Sand	>0.05mm	43.9	% Sand	>0.05mm	48.5
% Silt	0.05 to 0.002	48.1	% Silt	0.05 to 0.002	46.7
% Clay	<0.002mm	8.0	% Clay	<0.002mm	4.8
	66 to 92 cm			**61 to 92 cm**	
% Sand	>0.05mm	54.6	% Sand	>0.05mm	38.1
% Silt	0.05 to 0.002	41.3	% Silt	0.05 to 0.002	45.6
% Clay	<0.002mm	4.1	% Clay	<0.002mm	16.4
	137 to 152 cm			**142 to 152 cm**	
% Sand	>0.05mm	37.0	% Sand	>0.05mm	37.9
% Silt	0.05 to 0.002	43.9	% Silt	0.05 to 0.002	42.1
% Clay	<0.002mm	19.1	% Clay	<0.002mm	20.1
	244 to 259 cm			**244 to 257 cm**	
% Sand	>0.05mm	38.1	% Sand	>0.05mm	42.9
% Silt	0.05 to 0.002	41.2	% Silt	0.05 to 0.002	38.9
% Clay	<0.002mm	20.7	% Clay	<0.002mm	18.2

The Btg horizons just below the E horizon have higher clay content and are more cohesive in moist conditions. Given the greater clay content, these horizons have a lower hydraulic conductivity and act as a lower confining layer to the water in the E horizon. There are substantial amounts of hydrous-oxides in concretions and mottles in these horizons. This indicates a variable water table giving changing redox conditions. The Bg3/C horizon is possibly a relic soil or partially weathered parent material. This horizon is less cohesive than the material above, but also contains some mottles and concretions. The lowest layer of the cores is made of very cohesive clean clay that occasionally had a stringer of medium to fine grained sand. With the exception of the sand stringers, this layer is effectively an aquitard, with almost no hydraulic conductivity. This layer was used as a stopping point in four of the six cores taken. In

borehole 6 the core stopped at a depth of 2.7 meters, and borehole 2 was stopped at refusal when it hit buried wood at a depth of 0.7 meters.

Hydrogeologic Characterization

In order to determine the hydrologic properties of the sinkholes and the hydraulic conductivity of the site, infiltration tests were carried out. Tests were run at several locations, inside and outside of sinkholes, using a double ring infiltrometer manufactured by Turf Tec Inc. The test was setup by penetrating the two rings of the infiltrometer into the soil to be tested up to a stop ring, and then the rings were filled with water. At the instant the rings were full of water a timer was started as the water was allowed to drain from the rings. These tests were repeated at each location until the drainage rate had leveled off as the soil approached saturation (Table 3). At the saturation level the infiltration rate is equal to the saturated hydraulic conductivity of the soil.

Table 3. *Saturated hydraulic conductivity data.*

Data from the Soil Survey of Liberty County, Texas (Griffith et al., 1996)		Field data from double ring infiltrometer
Depth (cm)	cm/hour	Outside of sinkholes
0 to 13	1.5 to 5.1	5.2 to 6.6 cm/hour
13 to 89	1.5 to 5.1	Within Sinkholes
89 to 152	0.15 to 0.51	61 to 269 cm/hour

The data shown in Table 3 clearly shows a much higher rate of infiltration within sinkholes than outside of them. The first infiltration test was conducted in an area far from any sinkholes where the saturated infiltration rate was 6.5cm/hour. The

infiltration rate measured just outside of a sinkhole was 5.2cm/hour. Where as, within the sinkhole the infiltration rate was 61cm/hour. At another sinkhole the infiltration rate was 269cm/hour. The substantially higher saturated hydraulic conductivity of the sinkhole supports the idea that they are related to some kind of hydraulic conduit. The estimated hydraulic conductivity of the study site is compared to the published value for the Waller Soil in Table 4. A conservative value of 5 cm/hr for hydraulic conductivity will be used for calculating flow rate and velocity.

The hydraulic gradients were determined from three nests of piezometers. Each piezometer consists of 1.5 in (3.8 cm) diameter PVC pipe enclosed with an end cap. The last 15 to 30 cm of these pipes had 1mm slots cut into the pipes to allow water to pass through. At each of these nests a piezometer was installed near the bottom of a borehole (approximately 2.5 m), and surrounded with industrial sand in the screened interval. On top of this excess recovered material was used to fill until a depth of approximately 1.8m. then bentonite granules were placed to hydraulically seal off the piezometer below. At approximately 1.4m another piezometer was placed and the burial procedure was repeated with a final bentonite seal at the surface. The total hydraulic potential, or hydraulic head, was determined by inserting a water sounding probe into the piezometers. The hydraulic gradient is the difference in two potentials over the distance separating the measuring points. Each nest allow for the determination of vertical horizontal hydraulic gradients. The three nests together allow for the calculation of horizontal hydraulic gradients.

There were two distinct depths at which piezometers were installed, approximately 2.5 meters and 1.4 meters (Table 4). The deep peizometer in well nest number 3 did not have a measurable water level, where as, the other two well nests had over two meters of water above the screened interval. This could be interpreted in two ways: 1) there is an anomously large gradient in the lower part of the soil, or 2) there is a leak from above in well nests 1 and 2. The second option is quite possible given that one of these wells was placed in an area of relatively high ion concentration that could cause flocculation and shrinkage of the bentonite seal allowing water to pass. Also, during the initial coring of the wells the lower interval seemed relatively dry. Therefore the data from the deepest piezometers was ignored for calculating horizontal gradients.

Table 4. *Hydraulic head and gradient data.*

Well nest no. 1 (Borehole # 4)

(Located 93.55m S, 6.82m E, at an elevation of 1.195m relative to the benchmark) 1/30/2003

Piezo. No.	Screened Interval in meters	Depth to Water in meters	Adjusted Head in meters	Vertical Gradient from piezo. below
Piezo. #1	2.53 to 2.23	0.14	1.05	
Piezo. #2	1.37 to 1.22	0.09	1.1	0.050
Piezo. #3	0.46 to 0.30	0.08	1.11	0.030

Well nest no. 2 (Borehole # 5)

(Located 48.51m S, 2.85m E, at an elevation of 0.785m relative to the benchmark) 1/30/2003

Piezo. No.	Screened Interval in meters	Depth to Water in meters	Adjusted Head in meters	Vertical Gradient from piezo. below
Piezo. #1	2.44 to 2.13	0.22	0.56	
Piezo. #2	1.40 to 1.25	0.17	0.61	0.057

Well nest no. 3 (Borehole # 6)

(Located 47.98m S, 28.68m W, at an elevation of 0.89m relative to the benchmark) 1/30/2003

Piezo. No.	Screened Interval in meters	Depth to Water in meters	Adjusted Head in meters	Vertical Gradient from piezo. below
Piezo. #1	2.53 to 2.23	no reading		
Piezo. #2	1.37 to 1.22	0.21	0.68	N/A

Horizontal Hydraulic Gradient

(Calculated from the piezometers with a screened interval of 1.22 to 1.40 meters depth.) 1/30/2003

Gradient:	0.0109	Direction:	N7.2E

From the product of the hydraulic conductivity (5cm/hr.) and gradient (0.01), the specific discharge is $1.5x10^{-7}$m/sec. The porosity of fine sand can range from 26 to 53 percent and silts can range from 34 to 61 percent (Domenico and Schwartz, 1998). A conservative value of 34 percent was used for the porosity of the soil at this site. With this assumption, the velocity of the ground water is $4.4x10^{-7}$ m/sec or 14 m/year. The hydraulic gradients and velocity are relatively low, but do not preclude the possibility of piping. Piping usually takes advantage of an initial opening and pathway in which water velocity is much greater.

The data shows that there is a perched water table on top of the B soil horizons. This has several consequences. First, given that this water table is extremely shallow, the water levels will be strongly dependant upon precipitation and evapotranspiration. Thus, the gradients will be highly seasonal. Also, the water table and gradients will be strongly tied to topography and vegetation. Therefore, the hydraulic gradients at this site will be highly variable in space and time, and the calculation of hydraulic gradients, conductivity and ground water velocities only give an approximation of reality.

Discussion and Conclusions

The site investigation has led to the discovery of several anomalous characteristics of the site, which may help explain the process by which the sinkholes are forming. The geophysical investigation of the site led to several important discoveries including: the high apparent conductivity zone, most probably from a release of brine

from the nearby injection well, and the sinkholes are more common in areas of slightly elevated apparent electrical conductivity. Plus, the saturated hydraulic conductivity was 10 to 50 times greater in the sinkholes, which supports the idea that the sinkholes are related to a hydraulic conduit such as piping, but is not mutually exclusive to other explanations. Also, by comparing a set of cores within and outside of a sinkhole it was found that the core of the sinkhole soil is depleted in colloid size particles in the E-horizon and appears to be the primary horizon for volume loss. The depletion of colloid size particles is especially telling. Soil colloids, usually clay minerals, have strong cohesive forces, which bind soil together making it difficult to entrain by fluids. To deplete a soil of these particles and leave behind silts requires that either the colloids were dissolved from the soil or that the cohesive forces that prevent their entrainment were reduced. The break down in cohesion of the soil, also known as dispersion, could allow for the depletion of the colloids through piping. There are several triggers of dispersion including the addition of sodium to colloid surfaces. This particular dispersing agent may be found at this site from the interpreted oil-field brine contamination of the site. Contamination of the area that leads to dispersion fits with the guiding principle that some external pressure, most likely anthropogenic, has caused the site to become out of equilibrium. It also explains the relatively restricted region over which the sinkholes appear and their recent appearance, because the interpreted contamination is localized.

Alternatively to classic piping, dispersed colloids may have been removed from the soil by intergranular transport. Intergranular transport of dispersed colloids is

possible because of the small size of the colloids. Dispersed colloids could be deposited into the void spaces between coarse sediments resulting in a redistribution of soil volume with the subsurface that would otherwise be impossible without dispersing the sediment. In a similar case of piping without an apparent exit point, Higgens and Schoner (1997) researched sinkholes formed by the internal piping of fine-grained soil into coarse alluvium in alfalfa fields in central California. They found that the fined grained sediments of the soil could only be transported into the coarse alluvium below after extensive irrigation had increased the velocity of water flowing through desiccation cracks. Thus, piping was only possible after an anthropogenic change to the environment made the normally stable soil transportable. At the site in Cleveland, Texas, the most probable change to the stability of the soil resulted from sodium induced colloidal dispersion.

It should be noted that the geophysics and subsurface investigation failed to conclusively find neither well-developed soil pipes nor an internal or external sediment sink. The electromagnetic induction technique employed lacks the resolution to reliably sense voids, and cores are too sparse in coverage to find discrete subsurface pipes. The ground penetrating radar was not able to image features in the top meter of the soil because of antenna coupling with the ground. This is important because the loss of soil colloids from the core taken from within a sinkhole was greatest at a depth less than one meter from the surface.

CHAPTER III

INVESTIGATION OF POSSIBLE SOURCES OF SODIUM

Introduction

The site investigation has led to the hypothesis that the cause of the sinkholes is from sodium-induced dispersion. A high apparent electrical conductivity zone emanating from a waste brine injection well is interpreted to be a brine leakage, and is thought to be the primary source of sodium contamination. During interviews, a property owner claimed to have disposed of a bag of water softener in the area of the metallic debris. Water softeners often contain substantial amounts of sodium and are often used as dispersing agents in laboratory experiments. This release of the water softener could explain a small portion of the sinkholes around the debris, but it would not explain the other sinkholes distributed through out the site. In order to investigate the validity of this hypothesis several conditions must be first met. These conditions include: that it is possible for a brine release to reach the areas of the sinkholes, that the brine contains the ratios of sodium needed for dispersion, and that the soil have elevated sodium levels.

To satisfy the condition that the brine has a sodium ratio sufficient for dispersion, study of the chemical components of oil-field brine is needed. The exact chemistry of the oil-field brine contamination at the site is not available. Because, a sample of non-degraded oil-field brine is not available, previous works had to be relied upon. Oil-field brines can vary in salinity and composition from differences in source rock origin, rock-water interactions, and diagenetic history (Bazin, et al., 1997). Bazin and colleagues

(1997) compiled 58 different oil-field brine samples. It was found that oil-field brines have a significant portion of alkalinity (77.5mmol/l) and small portions of carbonates and sulfates. Thus the hydrogen activity of oil-field brine at surface conditions averages pH 7.8. The proportions of major cations are not too dissimilar from the composition of seawater given that most oil-field sources have a marine or marine-deltaic origin. The same study found that the average composition of major cations for brines was dominated by sodium ions (130.7mmol/l), where as calcium (1.6mmol/l), magnesium (1.3 mmol/l), and potassium (1.4mmol/l) are relatively small portions of an oil-field brine's total cation composition. Thus, if the high electrical conductivity zone is oil-field brine contamination, it most probably contains relatively large portions of sodium for possible dispersion.

The presence of the high electrical conductivity zone near the oil-field brine injection well is not proof that the zone was caused by a spill from the well, nor that it is high in sodium content. Investigations into whether the soil does have elevated levels of sodium and that the waste from the well could be transported into the area of the sinkholes are necessary.

Methods and Results

Background Sodium Levels

In verification of the conditions that the contaminant is sodium rich and it has affected the site background levels were first established. A commonly used soil parameter for the prediction of sodium-induced dispersion is sodium adsorption ratio

(SAR) (Aitchison and Wood, 1965). SAR is defined by the following equation (All concentrations are in mEq/l).

$$SAR = [Na^{+}]/(\sqrt{\frac{[Ca^{2+}]+[Mg^{2+}]}{2}}$$

SAR is loosely based on ion exchange between the ratio of sodium, calcium, and magnesium in aqueous solution to the ratio of sodium adsorbed to the surface of soil colloids. SAR values were compared to exchangeable sodium ratio (ESR), defined as the actual ratio of sodium to other adsorbed ions on mineral surfaces (Bresler et al., 1982). The empirical relationship of SAR to ESR is given by the following equations:

$$SAR = \frac{(ESR + 0.0126)}{0.01475};$$
$$ESR = \frac{ES}{(CEC - ES)}.$$

where ES is the exchangeable sodium(Meq/100g). This empirical equation allows one to compare ratios for sodium extracted from the aqueous soil phase to data for ratios of sodium extracted from mineral surfaces. Higher values of SAR represent larger portions of sodium in the soil aqueous phase. Early researches cite SAR values as low as 5 for the threshold above which sodium-induced dispersion and piping may take place (Aitchison and Wood, 1965). Soil with SAR values greater than 13 are considered to be a sodicity hazard (Hallmark, 2003).

Expected values of SAR, from similar soil found in the region, were calculated from mineral extractable cation data to act as a guide to background SAR values (See Tables 5 and 6). To establish these expected SAR values for the soil at the study site,

data from the NSSC Soil Survey Laboratory database. (Soil Survey Staff, 2003) was used. Unfortunately, the Waller- Dallardsville soil that is found at the study site was not found in the NSSC Soil Survey Laboratory database. Instead soil with nearly the same soil classification, geologic setting, and climate were used to act as a guide. The predicted SAR values for these soil did not exceed 3, so values of 4 or greater may be considered anomalous for soil of this type.

Table 5. *Soil Characterization data for Merryville soil.*
Classification: Coarse-Silty, Siliceous, Thermic Typic Glossudalf
Sample Location: Beauregard Parish, Louisiana 3/4 of a mile east of Merryville

	NH_4OAC Extractable Bases							Calculated	
Depth	Ca	Mg	Na	K	Sum	CEC	pH	**ESR**	**SAR**
cm		Meq/ 100g			Bases				**Predicted**
0 to 10	0.4	0.2	--	tr.	0.6	4.5	4.1	**0.0E+00**	**1**
10 to 24	0.3	0.1	tr.	tr.	0.4	2.7	4.4	**0.0E+00**	**1**
24 to 45	0.6	0.2	tr.	tr.	0.8	3.5	4.6	**0.0E+00**	**1**
45 to 65	0.9	0.5	tr.	tr.	1.4	3.8	4.8	**0.0E+00**	**1**
65 to 90	2.1	1.3	0.1	0.1	3.6	8.4	4.6	**1.2E-02**	**2**
90 to 122	2.9	2.0	0.1	0.1	5.1	12.1	4.5	**8.3E-03**	**1**
122 to 140	2.3	1.4	0.1	0.1	3.9	8.9	4.8	**1.1E-02**	**2**
140 to 184	0.2	0.2	tr.	--	0.4	1.0	4.7	**0.0E+00**	**1**
184 to 216	0.3	0.2	--	tr.	0.5	1.1	4.7	**0.0E+00**	**1**
216 to 250	0.3	0.3	--	tr.	0.6	1.2	4.9	**0.0E+00**	**1**

Source of data except ESR and SAR: (Soil Survey Staff, 2003)

Table 6. *Soil Characterization data for Splendora soil.*
Classification: Fine-Loamy, Siliceous, Thermic Fragic Glossudalf
Sample Location: Montgomery County, Texas, 6.1 miles south of I45 and HW105

	NH_4OAC Extractable Bases							Calculated	
Depth	Ca	Mg	Na	K	Sum	CEC	pH	**ESR**	**SAR**
cm		Meq/ 100g			Bases				**Predicted**
0 to 10	2.5	0.9	tr.	tr.	3.4	6.2	4.8	**0.0E+00**	**1**
10 to 25	1.0	0.4	tr.	tr.	1.4	2.2	5.3	**0.0E+00**	**1**
25 to 51	1.6	1.5	tr.	tr.	3.1	6.9	4.6	**0.0E+00**	**1**
51 to 81	1.6	1.6	tr.	tr.	3.2	6.6	4.6	**0.0E+00**	**1**
81 to 117	1.5	1.8	0.1	0.1	3.5	6.4	4.8	**1.6E-02**	**2**
117 to 142	1.4	1.9	0.1	0.1	3.5	6.0	4.9	**1.7E-02**	**2**
142 to 175	1.3	2.0	0.1	0.1	3.5	5.8	4.8	**1.8E-02**	**2**
175 to 206	1.2	1.9	0.2	0.1	3.4	5.4	4.8	**3.8E-02**	**3**
206 to 241	2.7	2.8	0.3	0.1	5.9	8.4	4.6	**3.7E-02**	**3**

Source of data except ESR and SAR: (Soil Survey Staff, 2003)

Sodium Adsorption Ratios at the Study Site

With background levels for sodium adsorption ratio established the next step is to analyze the SAR levels in the soil samples from the study site. Nineteen different samples representing 4 different depth intervals and 5 different core locations were selected. In order to determine SAR values, standardized laboratory procedures of the Texas A&M University Soil Characterization Laboratory were used. Each soil sample was first air-dried and then crushed until the soil passed through a 2mm sieve. From each sieved sample, two 100g portions of thoroughly mixed soil were then measured and set aside. These 100g samples were then mixed with water until a saturated paste was made, and were allowed to sit for 24hrs. After which time, the water from the paste was extracted with vacuum extractors. Small portions of the extracted water were analyzed with an atomic absorption instrument for sodium, calcium, magnesium, and potassium.

The remaining fluids were analyzed for electrical conductivity (EC). The pH of each soil sample was determined using 1:1 soil to water mixture from the unused portions of the sieved soil. The results of this analysis, as well as the calculated SAR values, are given in Table 7 with respect to core locations and depth intervals. The location of each borehole is given on Figure 9.

Table 7. *Soil chemistry data for the Cleveland site.*

Borehole 4		Water Soluble Ions							
Sample	Depth	Ca	Mg	Na	K	Sum	**SAR**	**Ph**	**EC**
	cm	Meq/L				Cations			**mmhos**
H4-4-8	10 to 20	0.5	0.2	8.5	0.1	9.3	**14**	**6.6**	**1**
H4-14-20	36 to 51	1.3	0.2	16.1	tr.	17.6	**19**	**6.3**	**1.9**
H4-20-28	51 to 71	2.2	0.3	18.7	tr.	21.2	**17**	**5.9**	**2.4**
H4-28-34	71 to 86	3.4	0.4	23.0	0.1	26.9	**17**	**5**	**3**
H4-52-58	132 to 147	2.1	1.5	19.6	0.1	23.3	**15**	**4.8**	**2.6**
H4-98-104	249 to 264	5.5	4.1	20.4	0.2	30.2	**9**	**5.3**	**3.4**
Borehole 1									
H1-6-10	15 to 25	0.4	0.2	1.2	tr.	1.8	**2**	**4.9**	**0.2**
H1-56-60	142 to 152	0.1	0.1	1.5	tr.	1.7	**5**	**6.1**	**0.2**
H1-96-101	244 to 257	0.1	0.1	1.5	tr.	1.7	**5**	**6.2**	**0.2**
Borehole 3									
H3-6-14	15 to 36	0.4	0.2	1.0	tr.	1.6	**2**	**5.3**	**0.2**
H3-54-60	137 to 152	0.2	0.1	0.9	tr.	1.2	**2**	**5.5**	**0.1**
H3-96-102	244 to 259	0.1	0.1	1.1	tr.	1.3	**4**	**6.1**	**0.1**
Borehole 5									
H5-7-14	18 to 36	0.4	0.2	0.8	tr.	1.4	**2**	**5.5**	**0.1**
H5-51-57	130 to 145	0.1	0.1	0.3	tr.	0.5	**1**	**5.4**	**0.1**
H5-96-102	244 to 259	0.2	0.4	0.6	tr.	1.3	**1**	**5.5**	**0.1**
Borehole 6									
H6-7-14	18 to 36	0.2	0.2	0.7	tr.	1.1	**2**	**5.1**	**0.1**
H6-56-62	142 to 157	0.1	0.1	1.7	tr.	1.9	**5**	**7.1**	**0.2**
H6-96-100	244 to 254	0.1	0.2	0.8	tr.	1.1	**2**	**6.4**	**0.1**
Borehole 2									
H2-18-24	46 to 61	0.3	0.2	0.4	0.1	1.0	**1**	**4.8**	**0.1**

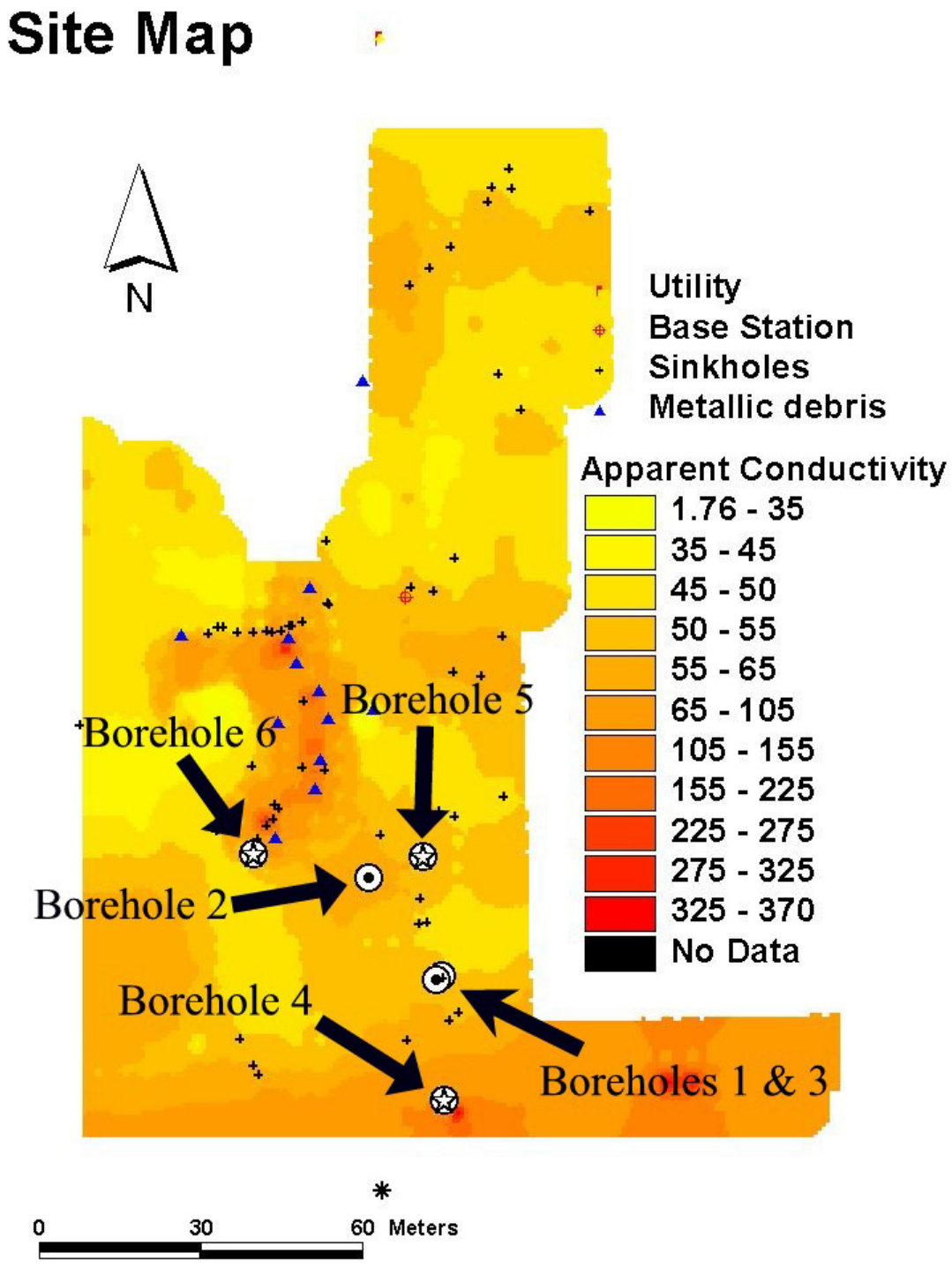

Figure 9. Locations of the boreholes relative to apparent EC and sinkhole locations.

Contaminant Transport Models

There are several modes of transport for the inferred oil-field brine contamination. This includes ground water transport or overland transport by surface runoff. An accurate model of contaminant transport requires considerable resources. Thus, a simple model that addresses whether the oil-field brine could have been exposed to the areas in which sinkholes are found is all that is desired. To make a useful model the boundary and initial conditions must first be established.

The boundary and initial conditions for contaminant transport in an aquifer are governed by: the hydraulic boundaries of the aquifer, the geometry and extent of the source, and the timing and duration of the contaminant release. The upper hydraulic boundary of the aquifer in this case is the water table surface, and the lower boundary of the aquifer is the clay rich B-horizon of the soil. It can be assumed that there are no lateral boundaries within the domain of the sinkholes, because of a lack of topographic divides and the lateral extent of the soil. The high conductivity zone transverses from west to east on the southern boundary of the study site, and there is a shallow ditch that runs parallel to this boundary that may provide the entry point for the contaminants into the shallow groundwater. This ditch runs nearly perpendicular the flow direction. The ditch itself is probably fed by brine overflowing the retaining walls surrounding the injection well during intense storms. This allows one to use a one-dimensional model, because the source is continuously distributed along one axis, and the water table and the B-horizon confine the vertical component leaving only one direction for flow.

There is a second possibility for the boundary conditions. The injection well complex could also act as a point source for the contaminant transport. In this scenario the vertical boundaries are the same, but the contaminant will have the ability to flow in the direction of advection as well as laterally. This dictates the need for a two-dimensional model as well. The time and duration of the exposure of the brine is difficult to establish. A single leak from the injection well may release brine into the groundwater for months with varying concentrations. A storm event or new leak could then replenish the ditch for more exposure. Because the timing of these releases is not known, the model will use a constant exposure through a decade in time. These conditions represent only a simplification of reality for the purpose of modeling possible outcomes and not an exact replica of the actual event.

The transport of the contaminant through groundwater can be estimated from the advection, mechanical dispersion, and retardation of the contaminant. The Orgatta-Banks analytical solution for 1-D contaminant transport in homogeneous media can be used to estimate contaminant movement (Dominico and Schwartz, 1998).

$$\frac{C}{C_o} = (\frac{1}{2})erfc[\frac{(R \cdot x - v \cdot t)}{2(\alpha \cdot v \cdot t \cdot R)^{1/2}}]$$

The equation describes the relative concentration (C/C_o) of a contaminant in distance (x) and time (t) with respect to the average velocity (v) of groundwater flow, mechanical dispersion (α), and the retardation (R). From the hydrogeologic data available, the estimate of the groundwater velocity of the contaminant is 4.4×10^{-7} m/sec or 14m/year.

An estimate of scale dependant contaminant dispersion can be made from a regression equation of data from numerous studies (Fetter, 1999).

$$\alpha = 0.83(\log L_s)^{2.414}$$

Where α is dispersivity and L is the distance from the source. Retardation (R) is a function of the amount of sorption of ions to mineral surfaces. The sorption of a cation such as sodium is dependant upon several characteristics of the ion and the mineral. Mineral surfaces exhibit a preference in what ions occupy exchange sites. This series, reprinted in Dominico and Schwartz (1998), shows the relative exchange preference of some of the cations believed to be in the oil-field brine.

$$Ca^{2+} > Mg^{2+} > K^{+} > H^{+} > Na^{+}$$

The amount of ion sorption to a mineral surface is also a function of its relative concentration in solution. By increasing the relative concentration of a cation in solution that cation will have more sorption to mineral surfaces. The sodium Na^{+} and calcium Ca^{2+} counter-ion exchange is a commonly studied example (Yariv and Cross, 1979, Olphen, 1991). The Na^{+} and calcium Ca^{2+} counter-ion exchange is described by the following equation:

$$k = \frac{(Ca^{2+})(NaX)^{2}}{(Na^{+})(CaX)}$$

where (k) is the ion exchange constant and (X) is the relative amount of that ion already absorbed to the mineral surface. Another important factor is the cation exchange capacity and the surface area of the minerals present at the site (Langmuir, 1997). The greater the cation exchange capacity and the surface area, the greater the sorption and

thus retardation of ions. Unfortunately, retardation of the contaminant requires specific data on the composition of the contaminant and the sorption capacity of the soil or column tests. Thus, retardation will only be considered in a qualitative manner.

The 2-dimensional analytical solution is given by the following equation:

$$\frac{C}{C_o} = (\frac{1}{4})erfc[\frac{(x - v \cdot t)}{2(\alpha \cdot v \cdot t)^{1/2}}] * \{erf[\frac{(y + Y/2)}{2(\alpha_y \cdot x)^{1/2}}] - erf[\frac{(y - Y/2)}{2(\alpha_y \cdot x)^{1/2}}]\}$$

where (*y)* is the lateral distance from the source, (*Y)* is the lateral dimension of the source, and (α_y) is mechanical dispersion in the *y* direction.

Contaminant transport by overland flow is governed by many of the same processes as groundwater transport. The velocities are much greater and are the dominant factor in surface transport. Unfortunately specific data on the velocity and duration of transport is not available. So, one-dimensional boundary conditions and initial conditions will be assumed for the surface water transport. The direction of surface flow can be determined from surface gradients, and the duration and velocity will be assumed to be sufficient to cover the entire study site in the time since initial exposure.

Contaminant Transport Results

The one-dimensional model for groundwater transport indicates that significant amounts of contaminant could cover the entire study site in as little as 10 years if not retarded (Figure 10). For, sodium there will be some retardation of transport because of sorption. Because of sodium's low selectivity for sorption and the relatively low CEC of

the soil at the site the retardation is probably relatively low (1-3). A retardation factor of 3 would cut the transport velocity by a third (Figure 11). For the two-dimensional model the contaminant plume would also cover the majority of the sinkhole area in about ten years. The area of the model-predicted plume has a strong correlation the area of the existing sinkholes (Figure 12).

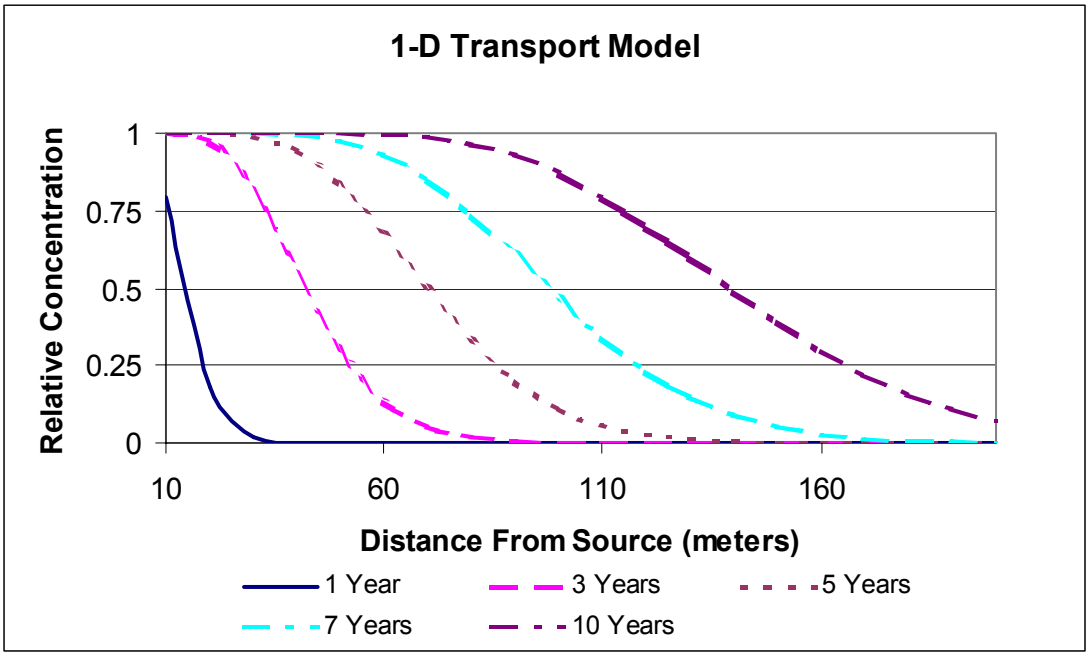

Figure 10. One-dimensional contaminant transport model assuming no retardation.

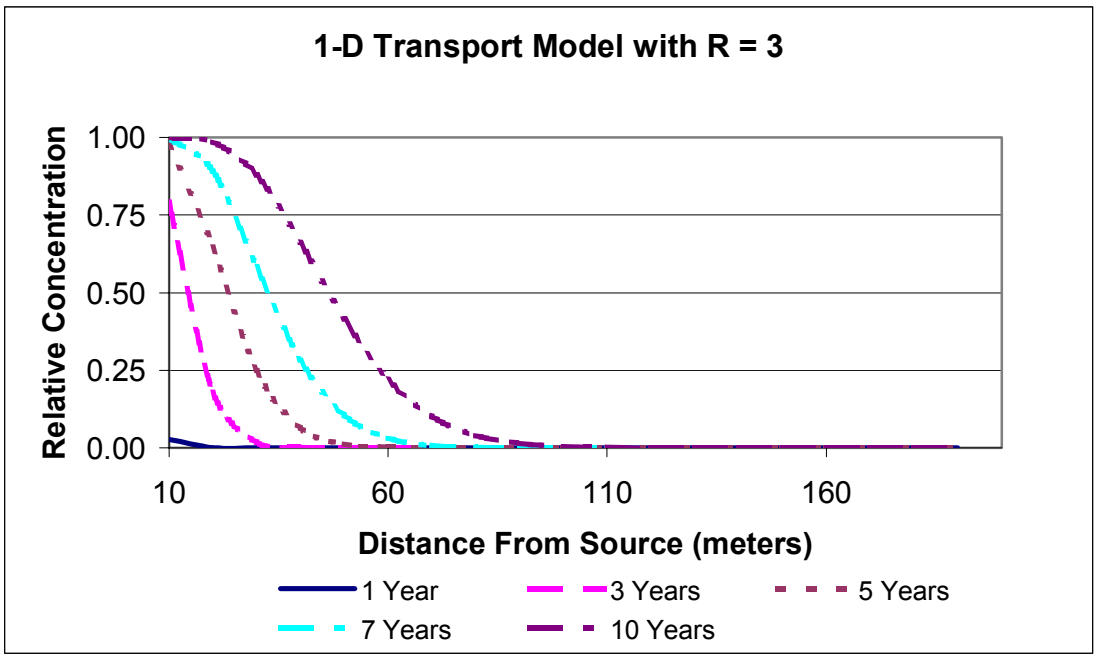

Figure 11. One-dimensional contaminant transport model assuming retardation of 3.

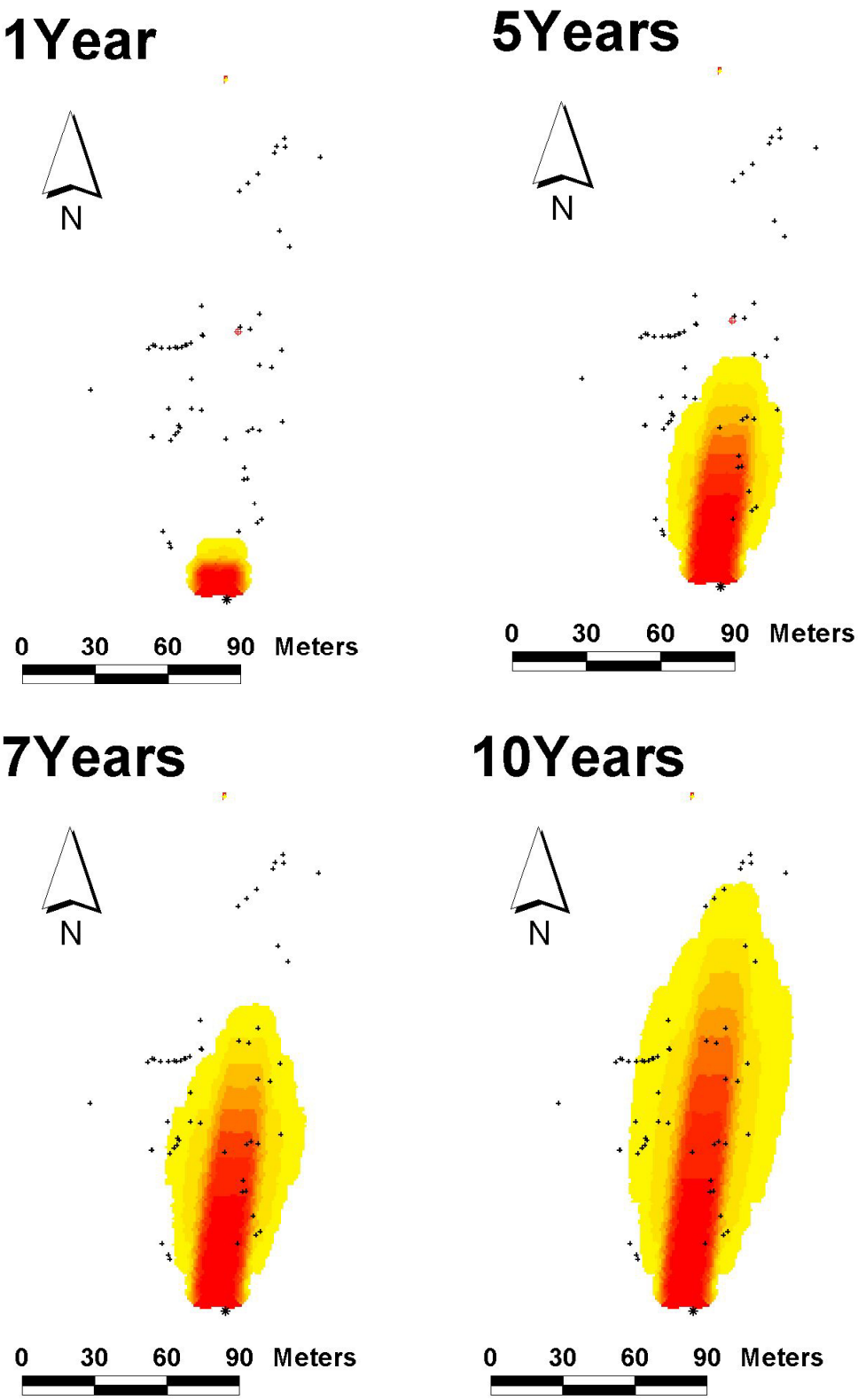

Figure 12. Two-dimensional contaminant transport model assuming no retardation.

The physical conditions for the surface transport of the oil-field brine into the area of the sinkholes are satisfied. The surface gradient, calculated from the surface points of the well nests, is 0.015 directed N32E. The drainage pattern at the site also trends in a NNE direction with some man-made drainage trending to the north. The transport velocity for overland flow will be much greater than the groundwater transport velocities. Significant accumulations of sodium could affect the site after a single strong rainstorm event.

Model Assumptions and Limitations

The models of the contaminant transport are very coarse and only indicate that, given some of the sites properties, the possibility of the contaminant reaching the area of the sinkholes exists. The initial conditions for the groundwater models use continuous sources for the contaminants. A long duration pulse or a series of pulses may be closer to the truth. Because there is not a confining layer above the contaminant, precipitation will dilute the concentration of brine in the groundwater. The timing of the initial release of the oil-field brine is not known. Also, the groundwater velocities are strongly dependant upon precipitation and evapotranspiration. In drought conditions the shallow aquifer may dry stopping transport completely, and in wet conditions the water velocities may be higher than those used in the model. Plus, natural heterogeneity of hydraulic conductivity, hydraulic gradient, mineral sorption and contaminant concentration will all affect the actual transport of the contaminant.

Discussion and Conclusions

The contaminant transport models built from the data of the subsurface and hydrologic investigations shows that the oil-field brine could have affected the area of the sinkholes. The distribution of higher electrical conductivity in the southern end of the site is close to what one would expect from brine being introduced from the drainage ditch in one-dimensional flow. Other areas of slightly higher electrical conductivity could be attributed to point source releases of brine or overland runoff transport. The actual transport mechanisms are probably a combination of the ones discussed herein and are also much more complex.

The data used for establishing background levels indicates that under normal conditions SAR should be very low, less than four. There is little surprise that the high conductivity plume at the site is from brine that has a high sodium content. However, the areas outside this high conductivity plume have also been affected by the same contamination.. Borehole 4 is centered within the high conductivity zone delineated from the geophysical survey. The SAR values, as high as 19, well exceeded the threshold for sodic conditions. This data clearly shows that the contaminant is rich in sodium as one would expect from oil-field brine, and may be sufficient to cause dispersion. Borehole 1 is located just outside the high conductivity zone within one meter of a sinkhole. The SAR values of the deeper two samples meet the minimum dispersion threshold value of 5 and exceed the expected background levels. Borehole # 3, which is located within a sinkhole one meter away from borehole #1, has values of EC and SAR that are strikingly different from borehole #1 just 1 meter away. This

difference is interpreted to be from the removal of ions and colloidal particles during piping or leaching from rapid infiltration. The SAR values neither indicate dispersion hazard nor significantly differ from expected background levels. Borehole 5 is located approximately 50 meters north of boreholes 1 and 3. The SAR and pH values are within the expected range for background levels. Borehole 6, which is located 50 meters west of borehole 5, is in a depressed area of the site near several sinkholes. The SAR values are higher than the expected background levels, and the SAR meets the minimum threshold for sodium-induced dispersion. It should be noted that the values expressed here reflect current conditions and may have been higher in the past.

The intent of this investigation was to find if the high conductivity zone contained elevated levels of sodium and a possible source of sodium. It was not designed to prove beyond all doubt that the source came from the oil-field brine injection well. Although highly unlikely, other sources of sodium could be responsible for the contamination of the site. Other sources include seawater and water softeners. Another chemical test, beyond the scope of this thesis, is that oil-field production brines have an elevated ratio of bromide to sodium (Whittemore, 1995). Plus, brines from oil-field production often contain volatile organic compounds such as benzene at much greater content than natural waters (Bair and Digel, 1990).

CHAPTER IV

STUDY OF THE DISPERSIVE BEHAVIOR OF COLLOIDS IN A HUMID ENVIRONMENT

Introduction

Previous works have shown that dispersed colloids cause: decreases in hydraulic conductivity (Shainberg, et al., 1980), piping erosion, slope failure (Durgin, 1984), degradation of soil-field productivity (Rengasmy, et al., 1984), increased erosion (Durgin and Chaney, 1984), and increased potential for transport of adsorbed contaminants on clay colloids (Dominico and Schwartz, 1998). In the study of natural colloid dispersion, sodium ions have been linked to the dispersion of soil colloids. This dispersing agent is also commonly associated with anthropogenic activities. Sources of these contaminants that come to mind include: road salt, saline irrigation waters, oil-field brines, waste from the dewatering of coal mines, and water from the depressuring of coal-bed methane production wells. The presence of elevated levels of sodium does not necessarily lead to the conclusion that sodium induced dispersion has in fact occurred. Within the geomorphology community, sodium induced dispersion is popularly thought not to be an important factor in humid soil (e.g. Jones, 1990). Also, there is no precedent of waste brine causing dispersion in the scientific literature. Therefore, a careful investigation is needed into whether increased levels of sodium most probably from waste brine can lead to increased dispersion in a soil of a humid environment.

Elevated sodium levels, most probably from the release of oil-field brine, are found in conjunction with sinkholes attributed to piping erosion at a site south of

Cleveland, Texas. oil-field waste brine, containing large concentrations of salts, is a common contamination problem in the U. S. Gulf Coast region (Barrett, 2002). This relatively common problem introduces sodium ions into the natural environment that may lead to the dispersion of clays and the associated problems, but has not been formally investigation. The research herein is focused on determining if the elevated sodium levels that were delineated during geophysical and soil characterization are in fact leading to increased soil dispersion in this humid setting.

Geochemical Setting

The study site is in a humid setting, the average annual precipitation is 53.56 inches (136.0 cm), and the average daily temperature ranges from a low of 49.8F° (9.89°C) in January to a high of 82.7 F° (28.2°C) in August (Griffith et al., 1996). The site is situated on the East-Texas-Coastal Plain. The underlying geology is the Pleistocene Lissie Formation, which is interpreted to be flood plain and delta plain deposits. The soil is very well developed and highly weathered. The soil at the study site is classified as fine-loamy, siliceous, thermic typic glossaqualfs named Waller soil (Griffith et al., 1996). The soil is flooded during the winter months with shallow groundwater. The pH of the soil ranges from 4.8 to 7.2.

The mineralogy of the soil is indicative of highly weathered sediments. An X-ray diffraction analysis of bulk soil samples indicates that the soil was dominated by quartz, and the other minerals were undistinguishable from one another. Fortunately, the National Soil-Survey-Center Soil-Survey-Laboratory's database (Soil Survey Staff,

2003) provided clay mineralogy of a soil, Splendora Soil, sampled in adjacent Montgomery County that has very similar characteristics. Their analysis by thermal DTA found that kaolinite ranges from 21%-38% of the colloid size fraction, and x-ray analysis found very small to small peaks for montmorillonite and small to medium peaks for montmorillonite-chlorite. Samples of the soil collected during fieldwork have yellow to red-orange mottles or staining, and red-orange to black concretions up to 3 cm in size. These mottles and concretions are interpreted to be iron, manganese and aluminum hydrous-oxides. Given the acidity and probable mineralogy of the soil, the soil colloids are expected to be variably charged with relatively low CEC and surface area.

Chemical Theory

Soil colloidal particles are very small (<2 microns) and posses very little strength (Olphen, 1991). However, soil colloids have electrostatic attraction between particles as well as Van der Waal attractive forces. These interactions of colloid minerals in a geologic system make them very cohesive and difficult to entrain. A breakdown in this attraction, called dispersion, makes the colloids highly erodible and transportable. An understanding of a basic model for the forces governing the interaction of colloids is beneficial for understanding the process of dispersion.

Clay minerals, a common colloid, have a net negative charge from isomorphic substitutions, and some positive charges from broken bonds and lattice imperfections (Olphen, 1991). Many other colloids such as hydrous-oxides can have either positive or negatively charged surfaces depending strongly on pH (Langmuir, 1997). Oppositely

charged colloids have electrostatic attraction, where as similarly charged colloids have electrostatic repulsion. Colloids also have attraction from Van der Waals forces (Olphen, 1991). These attractive forces can be overcome by altering the ions in the diffuse-double layer and bulk solution chemistry. The diffuse-double layer is made of ions and water molecules that are attracted to the surface charge of colloids, but also made diffuse by diffusion forces opposing the concentration of ions in a localized area (Güven, 1992). The repulsive forces of the diffuse-double layer are from the osmotic pressure that is created when two particles with high concentrations of ions in their respective diffuse-double layers interact (Güven, 1992). Thus any change in the colloid chemistry that weakens the electrostatic attractions and or increases double-layer repulsion will increase the potential for dispersion.

A solution containing sodium ions affects the dispersibility of clays in several manners. The specific cations that occupy the diffuse-double layer depend on the relative concentration of that cation in solution, the size of the cation, and the charge. The cations that occupy the diffuse-double layer can be changed through counter-ion exchange. By making conditions more favorable for a cation to replace another, it is possible to change the relative concentration of a cation on the clay surface. Favorable conditions are achieved by increasing the concentration of a cation in solution. The Na^{+} and calcium Ca^{2+} counter-ion exchange is described by the following equation:

$$k = \frac{(Ca^{2+})(NaX)^{2}}{(Na^{+})(CaX)}$$

where (k) is the ion exchange constant and (X) is the relative amount of that ion already absorbed to the mineral surface.

Changing the relative concentration of certain cations in the diffuse-double layer of clay can have significant effects on the repulsive forces between clay minerals. Calcium has a 2^+ charge and is held tightly to the clay face in the diffuse double layer, where as sodium has a 1^+ charge and is relatively small. This means more sodium cations can occupy the diffuse-double layer, and the sodium ions are not as tightly held to the clay surface given its lower charge. These two factors extend the range of diffuse-double layer repulsion by extending the diffuse-double layer through increased osmotic pressure and the weaker ion-surface attraction. Thus, a solution high in sodium will lead to cation exchange favoring sodium in the diffuse layer, which in turn increases inter-colloid repulsive forces.

A feedback effect of waters containing high concentrations of sodium is that high concentrations of ions can decrease dispersion. Higher ionic strength, measured by electrical conductivity (EC), mitigate the diffusion of the double layer by cutting down on the concentration gradients between the ions in the diffuse double layer and that of the bulk ion concentration in the water (Olphen, 1991). This allows electrostatic attraction between the clay and the cations to rule, collapsing the diffuse-double layer. The collapsed diffuse-double layer limits the effective range of osmotic repulsion allowing Van der Waals forces to rule.

Also, naturally occurring dissolved organic matter has also been shown to cause dispersion of soil colloids. Organic anions and cations, such as tannates and amine salts, can effectively reverse the charge of a colloid's surface, which can prevent electrostatic attraction between otherwise oppositely charged surfaces (Olphen, 1991). Naturally

occurring organic acids from the decay of tree roots has been shown to promote kaolinite dispersion by reversing its surface charge (Dugin and Chaney, 1984).

The surface charge of many colloids, and thus electrostatic attraction or repulsion of particles, can also be dependant upon pH. This is an especially important factor for oxides, hydrous-oxides and clays with broken bonds or lattice imperfection. At higher pH values OH^- complexes dominate surfaces leading to negative charge, and at lower pH values H^+ complexes dominate surfaces leading to positive charges (Yariv and Cross, 1979). The specific pH levels at which a colloid particle reverses charge is known as the point of zero charge (PZC). Table 8 shows the pH of charge reversal, also called the point of zero net proton charge, of some common soil minerals. The electrostatic surface potential can increase or decrease as pH changes, and is described by the following equation (Güven, 1992).

$$\Psi_o(mv) = 59.2[pH_{pzc} - pH]$$

Table 8. *The pH of the point of zero net proton charge (PZNPC) of some soil minerals.*

Solid	PH of PZNPC	Solid	PH of PZNPC
SiO_2 (quartz)	1 to 3	Mn(II) manganite	1.8
SiO_2 (amorphous)	3.5	MnO_2 (birnessite)	1.5 to 2.8
Montmorillonite	2 to 3	MnO_x (general)	1.5 to 7.3
Kaolinite	2 to 4.6	MnO_2 (cryptomelane)	4.5
Muscovite	6.6	MnO_2 (pyrolusite)	4.6 to 7.3
Fe_2O_3 (natural hematite)	4.2 to 6.9	MgO (periclase)	12.4
$Fe(OH)_3$ (amorphous)	8.5 to 8.8	$Al(OH)_3$ (gibbsite)	10
FeOOH (goethite)	5.9 to 6.7	$CaCO_3$ (calcite)	8.5

Source: Original table from Langmuir (1997).

In variably charged soil of heterogeneous minerals, electrostatic attraction will be an important factor at intermediate pH ranges. As pH moves away from the PZC of the bulk of the colloids, electrostatic repulsion becomes more prevalent (Seaman, et al., 1997). The change in pH, away from the PZC will result in an increase in the potential for dispersion.

Electrostatic attraction of oppositely charged colloids is stronger than osmotic repulsion forces and is thought to nullify the affects of sodium on dispersion, especially colloids with low CEC and surface area (Olphen, 1991). Thus, sodium induced dispersion is not thought to be important in soil of humid setting, which are typically variably charged with low-colloid CEC and surface area. This may be an unjustified deduction, because increased osmotic repulsion should still be a factor amongst like charged colloids in variably charged soil and thus contributing to loss of cohesion.

Conceptual Model

For sodium induced dispersion to occur the soil colloids should be loaded with Na^+ ions, but the pore water solution should have relatively low ion concentrations. This can be accomplished by immersing the colloids in a solution rich in Na^+ ions. The Na^+ will exchange with other cations on the mineral surfaces through counter-ion exchange. After this exchange has taken place, the optimal condition for dispersion will be when the remaining ions are flushed out of the pore fluids to reduce the effect of high ion concentrations on dispersion. At this site, the most probably source of the sodium is brine contamination, and the flushing of excess ions could be accomplished by rainwater

or fresh groundwater. Thus, dispersion may not take place until sometime after initial exposure of the contaminant. The research objective is to study the affect increased levels of sodium on dispersion in this particular setting by simulating this conceptual model.

Methods and Materials

Nineteen different soil samples from the study site were first analyzed, using standard soil characterization techniques, for parameters pertinent to dispersion (Chapter III). Each soil sample was first air-dried and then crushed until the soil passed through a 2mm sieve. From each sieved sample, two 100g portions of thoroughly mixed soil were then measured and set aside. These 100g samples were then mixed with water until a saturated paste was made, and were allowed to sit for 24hrs. After which time, the water from the paste was extracted with vacuum extractors. Small portions of the extracted water were analyzed with an atomic absorption instrument for sodium, calcium, magnesium, and potassium. From this data, sodium adsorption ratios (SAR) of each soil were calculated. The remaining saturated paste fluids were analyzed for electrical conductivity (EC). The pH of each soil sample was determined using 1:1 soil to water mixture from the unused portions of the same sieved soil samples.

In order to study the affect of increased sodium levels on dispersion, a procedure modeled after a method by Rengasamy et al. (1984) was used to simulate the dispersivity of the soil at the study site when exposed to rain water. The procedure follows the same principles as Rengasamy's method for spontaneous dispersion, except it was streamlined

for rapid measurements. To ensure representative samples, unused portions of the soil samples used in the SAR analysis were used. Dry soil samples were crushed to pass through a 2mm sieve. Forty-milliliter test tubes were filled with 25 milliliters of distilled water. Then 5 grams of the dried soil were slowly added to the water to minimize mechanical disturbance to the mixture. The soil-water mixture was left to sit for 12 hours to allow all silt and sand size particles to settle out. After the sitting period, 15ml of the fluid phase within the test tube was removed with a pipette, careful not to disturb sediment settled on the bottom. The removed fluid was placed into small sample jars for analysis of turbidity. Turbidity is the amount of suspended solids in water, and is measured with optical absorbance. Because dispersed colloids are stable as suspended solids in solution, turbidity is a measure of the amount of dispersion that has taken place. This procedure was repeated 3 times for each sample to account for variability that may arise in this modified procedure. As originally suggested by Rengasamy et al. (1984), turbidity levels where then divided by the percentage of colloid size particles, as determined from standard hydrometer analysis, to give the relative dispersion level. Also, The pH of the fluids was measured after analysis in the turbidity meter.

The relative dispersion data was compared with the data from the SAR analysis for statistical analysis. Rengasamy et al. (1984) successfully showed that dispersion could be modeled with SAR and EC as dependant variables with partial line slopes in Red Brown soil of Australia, a more arid setting. In another Australian study, modeled after Rengasamy's procedures, the linear partial slope of pH was a significant contributing factor to the prediction of dispersion (Little, 1989). As inspired by

Rengasamy and others (1984) and Little (1989), simple linear regression and stepwise multivariate linear regression analyses were performed to gain insight to the impact of SAR, EC and pH on dispersion in this setting.

A neural network was also used as an alternative data analysis method. The program was coded in C++ and compiled on a windows personal computer. The feedforward-multilayer neural network architecture with the sigmoid activation function was used. The optimal configuration consists of three layers with 4 input nodes, 9 hidden layer nodes, and 1 output node. The input vectors for this case consist of the soil parameters of EC, pH, SAR and the median depth of each sample, and the output vectors are the relative dispersion value for the respective input vectors. The back-propagation algorithm was used to train the neural network with the input and output vectors until a satisfactory level of convergence was reached.

Results and Discussion

Table 9 shows the result of the relative dispersion laboratory procedure.

Table 9. *Colloidal dispersion analysis data.*

Sample	Depth	A	B	C	Turbidity	Colloid	Relative	pH	SAR	EC
	cm		NTU's		Average	%	Dispersion		Saturated Paste	
H1-6-10	15 to 25	76.2	94.6	81.6	84.1	4.8	17.6	5.57	2	0.2
H1-56-60	142 to 152	165	140	172	159.0	20.1	7.9	6.23	5	0.2
H1-96-101	244 to 257	497	512	428	479.0	18.2	26.4	6.72	5	0.2
H2-18-24	46 to 61	295	222	213	243.3	10.1	24.2	5.95	1	0.1
H3-6-14	15 to 36	140	98.5	130	122.8	8.0	15.4	6.1	2	0.2
H3-54-60	137 to 152	211	255	204	223.3	19.1	11.7	6.31	2	0.1
H3-96-102	244 to 259	430	491	469	463.3	20.7	22.4	6.92	4	0.1
H4-4-8	10 to 20	110	159	111	126.7	2.5	51.6	6.96	15	1
H4-14-20	36 to 51	205	227	227	219.7	4.7	46.6	6.97	19	1.9
H4-20-28	51 to 71	96.2	85.8	80.3	87.4	7.0	12.6	6.56	17	2.4
H4-28-34	71 to 86	16.5	17.5	19.3	17.8	13.4	1.3	6.19	17	3
H4-52-58	132 to 147	8.62	8.52	7.5	8.2	22.6	0.4	6.23	15	2.6
H4-98-104	249 to 264	20	16.9	17.1	18.0	15.3	1.2	6.25	9	3.4
H5-7-14	18 to 36	246	264	199	236.3	6.5	36.4	6.23	2	0.1
H5-51-57	130 to 145	67.4	79.2	67	71.2	20.6	3.5	6.34	1	0.1
H5-96-102	244 to 259	310	258	353	307.0	27.2	11.3	7.02	1	0.1
H6-7-14	18 to 36	159	188	184	177.0	6.7	26.5	6.52	2	0.1
H6-56-62	142 to 157	316	234	321	290.3	16.7	17.4	7.12	5	0.2
H6-96-100	244 to 254	1318	805	1110	1077.7	15.9	67.9	7.22	2	0.1

Multivariate Liner Regression Analysis

In stepwise multivariate linear regression model, parameters are added one at a time to the regression to see if the model improves upon the addition of that variable. Model parameters are continuously added until no further improvement is found, or a predetermined level of fit is reached. The parameters that are added should be pertinent to the physics of the problem. In the initial model, step 1 in Table 10, a simple regression of turbidity verses SAR has a coefficient of determination of 0.000, and actually projects a negative slope. This result was not unexpected, as dispersion is

dependent upon SAR as well as EC. In the second step EC was added to the regression model, the R^2 value and residual standard deviation improved.

Table 10. *Results of step-wise multivariate regression for dispersion verses SAR, pH, and EC.*

Step 1 Turbidity vs. SAR

Variable	Parameter Estimate	Statistic	Value
Partial Slope SAR	-0.023	R^2	**0.000**
Intercept	21.323	Residual Std.Dev.	17.910
		SS(Residual)	6094.000
		MS(Residual)	380.897

Step 2 Turbidity vs. SAR and EC

Variable	Parameter Estimate	Statistic	Value
Partial Slope SAR	2.238	R^2	**0.306**
Partial Slope EC	-15.321	Residual Std.Dev.	14.920
Intercept	19.312	SS(Residual)	4230.000
		MS(Residual)	281.984

Step 3 Turbidity vs. SAR, EC, and pH

Variable	Parameter Estimate	Statistic	Value
Partial Slope SAR	1.441	R^2	**0.419**
Partial Slope EC	-11.046	Residual Std.Dev.	13.657
Partial Slope pH	15.384	SS(Residual)	3544.000
Intercept	-78.949	MS(Residual)	236.238

This model is an entirely inadequate fit of the data and theory. In another Australian study modeled after Rengasamy's procedures, the linear partial slope of pH was a significant contributing factor to the prediction of dispersion (Little, 1989). Because this particular soil is suspected of having variably charged colloids that are strongly dependant upon acidity, pH would be another appropriate model parameter to add. The electrostatic surface potential of colloids that are pH sensitive increase linearly as pH shifts from the point of zero charge. The electrostatic repulsion and double-layer

repulsion increase in proportion to electrostatic surface potential (Güven, 1992). The dispersion should increase as pH becomes greater than or less than the point of zero charge of the bulk of the soil minerals (Seaman et al., 1997). Knowing that kaolinite probably is the dominant colloid at the site, and that it's PZPNC is approximately 4.5 or less, dispersion should increase with pH values greater than 4.5. Because the pH values observed range from 4.8 to 7.2, a partial line slope may be an appropriate model for estimating dispersion from pH. Thus the third step uses a regression model that uses SAR, EC and pH has a coefficient of determination (R^2) of 0.419. This is a significant improvement, but still shows a lack of fit of the model to the data. The plot of residuals from this regression shows that the final data point with an extraordinarily high turbidity level as having the least amount of fit (Figure 13).

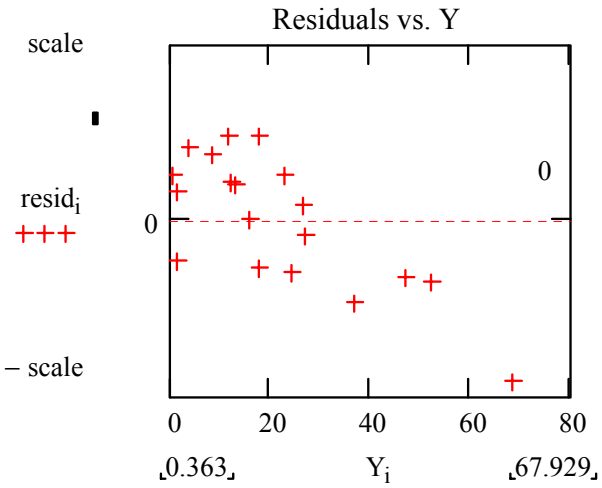

Figure 13. Plot of residuals against misfit of data (Y).

This value is treated as a high influence point and removed from the data set for further regression analysis summarized in Table 11. The model with the removed influence point in the next attempt resulted in an improvement in the R^2 value to 0.488. This is still not a satisfactory fit to the data.

Table 11. *Step 4 dispersion vs. SAR, EC and pH (Minus high influence point).*

Variable	Parameter Estimate	Statistic	Value
Partial Slope SAR	2.314	R^2	**0.488**
Partial Slope EC	-14.092	Residual Std.Dev.	10.374
Partial Slope pH	3.058	SS(Residual)	1937.000
Intercept	-4.583	MS(Residual)	138.357

Table 12. *Regression analysis of dispersion vs. SAR, pH, and EC at certain depth classes.*

Depth Class 1 (10 to 36cm depth)

Variable	Parameter Estimate	Statistic	Value
Partial Slope SAR	16.473	R^2	**0.967**
Partial Slope EC	-208.406	Residual Std.Dev.	2.413
Partial Slope pH	-10.919	SS(Residual)	29.112
Intercept	88.957	MS(Residual)	29.112

Depth Class 3 (130 to 157cm depth)

Variable	Parameter Estimate	Statistic	Value
Partial Slope SAR	1.114	R^2	**0.835**
Partial Slope EC	-8.333	Residual Std.Dev.	2.446
Partial Slope pH	9.250	SS(Residual)	29.909
Intercept	-52.359	MS(Residual)	29.909

Depth Class 4 (244 to 264cm depth)

Variable	Parameter Estimate	Statistic	Value
Partial Slope SAR	13.867	R^2	**0.863**
Partial Slope EC	3.560	Residual Std.Dev.	8.457
Partial Slope pH	174.023	SS(Residual)	357.568
Intercept	-1223.000	MS(Residual)	357.568

The lack of fit in the model is interpreted as a failure of the original model to take into account soil mineralogy and dissolved organic matter with respect to depth. Soil horizons with a higher amount of dispersion sensitive minerals and organic dispersing agents will yield a higher amount of dispersion under the same geochemical conditions. In response to this interpretation another set of attempts, summarized in Table 12, looked at the multiple regression model on data from similar depth classes. These models represent a drastic improvement on the fit on the model to the data, verifying that mineral and organic matter dependence is a very likely the source of the lack of fit problem. In natural soil forming processes specific minerals and organic compounds tend to variegate into soil horizons. Samples taken at the same depth of a soil will be similar with respect to mineralogy and organic content. Therefore, depth classes were introduced in the data analysis to help resolve the issue of variations in mineralogy and organic. Depth classes are qualitative data, which can be included in multivariate regression as treatments, using dummy variables as parameters in the model (Ott and Longnecker, 2001). The treatments, summarized in Table 13, were used in the following regression analysis yielded an R^2 value of 0.763 and is summarized in Table 14. This represents the best regression for the model with the data available.

Table 13. *Table of treatments*.

Treatment #	Treatment equivalent to:	if then	otherwise
Treatment 1	Depth Class 1 (10 to 36cm depth)	intercept	
Treatment 2	Depth Class 2 (36 to 86cm depth)	$x_4 = 1$ if treatment 2	$x_4 = 0$ otherwise
Treatment 3	Depth Class 3(130 to 157cm depth)	$x_5 = 1$ if treatment 3	$x_5 = 0$ otherwise
Treatment 4	Depth Class 4 (244 to 264cm depth)	$x_6 = 1$ if treatment 4	$x_6 = 0$ otherwise

Table 14. *Step 5 dispersion vs. SAR, EC, pH and treatments (Minus high influence point).*

Variable	Parameter Estimate	Statistic	Value
Partial Slope SAR	1.761	R^2	**0.763**
Partial Slope EC	-11.129	Residual Std.Dev.	7.069
Partial Slope pH	9.008	SS(Residual)	899.359
Treatment 1	-21.070	MS(Residual)	81.760
Treatment 2	-11.532		
Treatment 3	-8.27		
Intercept	-31.561		

At this point the question of whether or not the elevated sodium level has any statistical contribution to the prediction of dispersion in these soil, assuming the data and model available is appropriate. The null hypothesis tests whether there is a contribution of SAR to the prediction of the dispersion levels observed is null or is by chance alone. The alternative hypothesis is that there is a contribution to the prediction of dispersion from the SAR and it is not by chance alone. The test statistic, Student's t Test, yielded 2.356, which is greater than 2.201 for an alpha value of 0.05 and 11 degrees of freedom. This means that the null hypothesis can be rejected when one is willing to accept a 5% chance that the conclusion may be falsely accepted. One can accept the alternative hypothesis that SAR has some predictive power for relative dispersion beyond chance alone.

This second attempt, utilizing dummy variables, to evaluate dispersion as a function of pertinent soil parameters is weak at best. It does not properly account for the reason why mineralogy affects the regression models. Two different mineral

assemblages under the same geochemical conditions will have very different dispersive behaviors. Minerals, such as kaolinite, with low CEC and surface area are not expected to be as strongly influenced by high SAR values as other colloid minerals. Also, the changes in dispersive behavior of different minerals because of changing pH will vary depending on a mineral's PZC. The change in electrostatic potential from changing pH in turn changes the affect of sodium on dispersion. Thus, the parameters of pH, SAR and mineralogy do not act independently from one another and all linear statistical data analysis techniques are inappropriate because the dynamics of the problem are instead non-linear. At the same time the true interaction between these parameters are poorly understood. Therefore, a non-linear data analysis tool that is capable of dealing with an ill posed problem is needed.

Neural Network Analysis

Neural networks can deal with ill posed, non-linear problems. Neural networks are universal approximators of any function (Steeb, 1999). They are also "black box", so a detailed knowledge of the mathematics of physics of the problem is not needed. They are also advantageous because they can still recognize the underlying structure of noisy and incomplete data. Thus, neural networks are very useful for data analysis of natural systems where inherent heterogeneity limit the use of normal statistical methods or simple physical explanations.

Neural networks algorithms were developed from the study of animal learning, and thus behave more like brains than computers. Neural networks allow computers to

perform functions that involve the ability to make generalizations, recognition, and prediction. A typical neural network consists of a collection of interconnected nodes that communicate with each other, just as neurons in a brain. The back-propagation algorithm trains a neural network to associate a certain stimulus, or input, with an output. This is accomplished by adjusting the weight of connections between nodes in the network to minimize an error between the actual output and the desired output (Rumelhart et al. 1986).

All neural networks are made of multiple nodes that simulate neurons, and connections that simulate the dendritic connection of nerve cells. The most popular type of neural network is the multilayer feed-forward neural network. The feed-forward part of its name comes from the fact that inputs are sent through and proceed to the output front to back. This type has a network structure of three or more layers, each layer is made up of a certain type of node. The first layer is the input-node layer and the last layer is the output-node layer. The input layer has the same number of nodes as the number of entries of the input vector, and the output layer has the same number of nodes as the number of entries in the output vector. An input vector can be thought of as a question, and the output vector can be thought of as the answer for the respective question in the input vector. The layers in between are called the hidden layers. These layers act as the intermediate between the input vector and output vector. This additional step and the complexity of the connections is what allow multi-layer-neural networks to deal with complex problems. One of the most popular algorithms for training neural networks is the back-propagation method. The Back-propagation method

is a learning procedure for multi-layered, feed forward neural networks (Ooyen and Nienhuis, 1992). In the training phase, back-propagation attempts to match an input vector to an output vector. Back-propagation trains the neural network by changing the node interaction weights to minimize the error between the current output vector and the desired output vector of the network.

The input vectors for this case are the soil parameters of EC, pH, SAR and the median depth of each sample. The output vectors are the relative dispersion value for the respective input vectors. Depth was included to act as a type of analog-dumby variable for changes in mineralogy and dissolved organic content with respect to depth. This qualitative information was used with the "geologic" knowledge that minerals, organic ions, and geochemical conditions variegate in soil during soil formation into soil horizons. Thus the depth parameter qualitatively represents these changes in the soil. The back-propagation algorithm was run for 10,000 iterations reaching a least-squares error of 0.0056. In statistical terms the equivalent R^2 value would be 0.97.

In order to analyze the underlying pattern and dynamics of the data presented to the trained neural network, various sets of new input parameters within the interval of the training data were displayed to the network. Of the four input parameters, SAR, EC, pH and depth, three were held constant and one was varied. This was repeated for several depths to evaluate the interaction between mineralogy, dissolved organics and that particular parameter. The trained neural network output from these data sets were plotted to visually show the relationship of a particular input parameter on dispersion.

These output sets also provide an idea of the dynamics between the various factors affecting dispersion, although informally.

There are two additional reasons for this approach of studying the neural network including: the ability of the neural network to define the underlying patterns within the data, and the generalization ability of the neural network. In there present state neural networks, unlike statistical methods, lack a formal means of measuring uncertainty, level of training or confidence intervals. Despite the high level of convergence and fit to the data, there is the risk that the neural network failed to pick up on the correct pattern during training, or that it was over trained resulting in memorization of the data thus loosing its generalization ability. Therefore criteria must be set to judge how well the neural network accomplished its goals. The criteria for concluding that the network found the correct pattern from the data is that the output should reflect the chemical theory of dispersion, and there should be some correlation to the statistical results. The criteria for concluding that the neural network has the ability to make generalizations rather than just memorizing the data set is that the network should be able to deal with data it has never seen before, but within the range of its training set.

When all parameters were held constant except SAR the neural network showed an increase in the predicted levels of dispersion with increasing SAR values (Figure 14). This is just what would be expected from the theory of sodium-induced dispersion. It also reflects the same positive slope the statistical analysis provided. At various depths the SAR does not have the same exact result, suggesting that the changes in mineralogy and dissolved organic matter with depth have an influence on dispersion. The neural

network shows that increased sodium content is a very strong contributing factor to the dispersion of these soil samples.

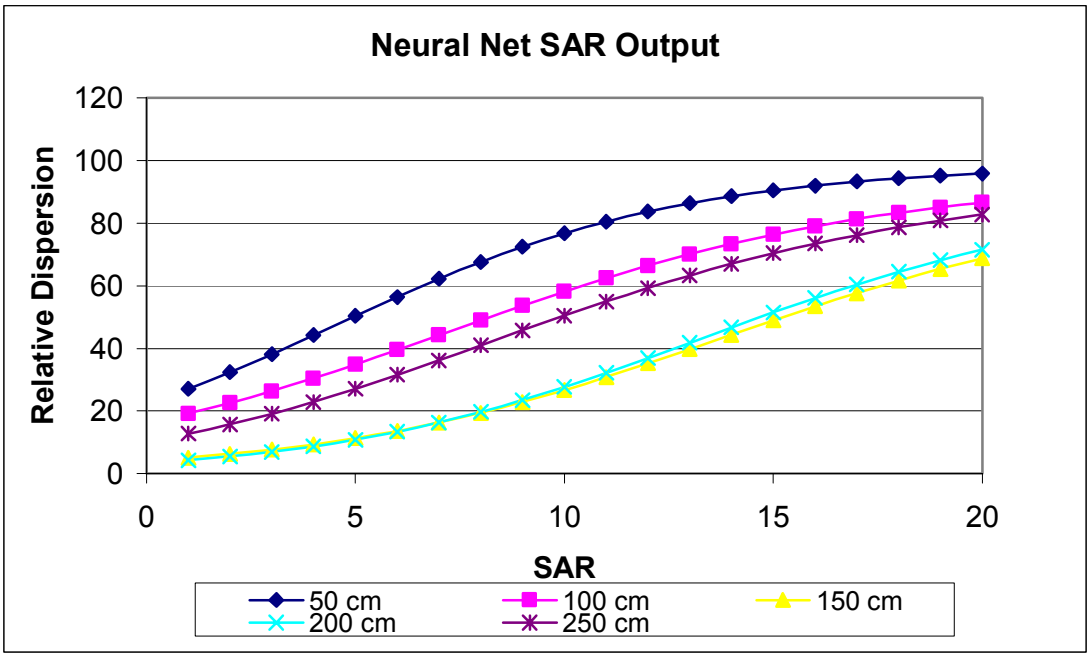

Figure 14. Dispersion levels for various levels of SAR with pH 6.5 and EC 0.2 dS/m.

In the study of EC, the neural network showed the expected decrease in dispersion with increased EC (Figure 15). This matches the chemical theory of the affect of ion concentrations on colloid dispersion. As with the SAR output from the neural network, the EC output showed a strong generalization ability and variation of dispersion with depth.

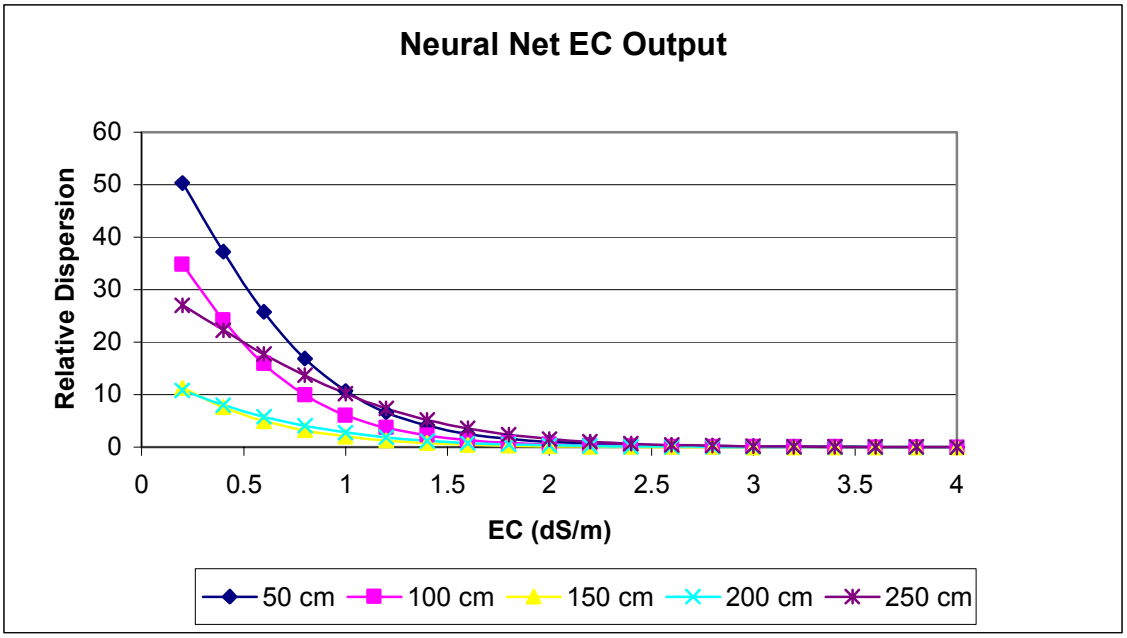

Figure 15. Dispersion levels for various levels of EC with pH 6.5 and SAR of 5.

The dynamics between dispersion and changing pH is not as simple as SAR or EC (Figure 16). When all other parameters were held constant except pH, the neural network showed that the predicted dispersion level has a strong dependence on the depth of the sample. This suggests that changes in pH have differing affects depending on the mineralogy and dissolved organic matter in the soil samples. This can be attributed to changes in electrostatic potential of the mineral and organic ions from changes in pH. This dynamic is what made linear data analysis tools relatively ineffective.

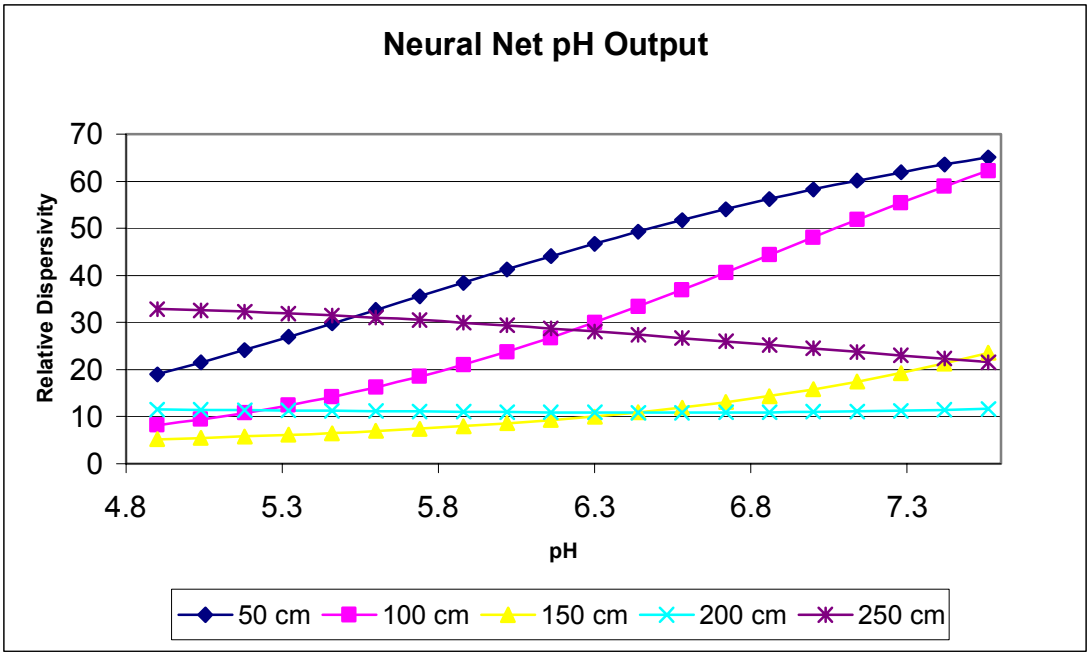

Figure 16. Dispersion levels for various pH levels with EC of 0.2 dS/m and SAR of 5.

In all, the neural network results reflected the chemical theory of colloidal dispersion indicating that it successfully found the underlying pattern within the data. Also, the smooth continuous plots of the output from the new input values show that the network has retained its generalization ability and has not been over trained.

Both the statistical and neural network analysis indicates that increased levels of sodium adsorption ratios lead to greater levels of dispersion. This provides the strongest evidence yet for contaminant-induced dispersion at this study site, and dispels myths that sodium is not an important factor on dispersion of humid climate soil. The opinion that sodium does not have an impact on dispersion in humid soil may stem from the influences of pH on dispersion or the difficulties in analyzing soil of this type with traditional statistical methods. It should be noted that in soil with lower pH levels than

studied here may have a positive surface charge, which would nullify the affects of sodium on dispersion. The rule of thumb for sodium-induced dispersion is not a matter of the climate a soil forms in but the pH and mineralogy of the soil of interest.

The soil data and analysis also strongly suggest that dispersion is the most likely cause of the sinkholes at the study site. During the initial site investigation it was noted that the E-horizon, centered at approximately 55cm, had experienced the greatest loss by volume. Also, this layer had a significant loss of colloidal size particles. From the neural network analysis the impact on dispersion from increased SAR and pH is strongest on this particular zone. This indicates that this zone is most sensitive to the influence of a contaminant. The coincidence of the soil loss of this layer and its dispersion sensitivity is interpreted as evidence that colloidal dispersion from a contaminant that increased SAR and pH lead to the soil loss and sinkhole development. Considering the sensitivity of this zone and the evidence that the bulk of loss is within this layer, any further analysis can focus on this particular zone.

Also, from the neural network analysis is becomes clear that the effect of pH on colloidal dispersion is dependant upon changes of mineralogy and organic content with depth. The analysis indicates that an increase in pH has nearly the impact on dispersion as increases in SAR. The pH ranges found from the experiments present here are noticeably higher, 4.8 to 7.2, compared to the 4.5 to 6.0 as reported in the Soil Survey of Liberty County, Texas (Griffith et al., 1996) for the same soil. Given that the data analysis indicates that an increase in pH causes an increase in dispersion, the cause of the increase in pH becomes an important consideration in the cause of dispersion at this

site. One idea is that the oil-field brine contamination may have led to an increase in pH of the soil at the study site. The brine may have disrupted soil biologic activity, decreasing CO_2 production and thus leading to higher soil pH (Herbert, 2003). Plus, oil-field brines are known to have high pH levels and contain portions of alkaline and carbonate which could cause a rise in soil pH. Also, soil reactions with the oil-field brine may have increased the pH in the soil at the site.

> "As the original saltwater in clastic strata is diluted and flushed, cation exchange decreases calcium and magnesium concentrations in solution, allowing contaminant dissolution of present carbonate minerals. Sodium-bicarbonate-type waters often result in clastic sediment aquifers once the original salinity decreases to a point where the chloride is less than the bicarbonate concentration (Whittemore, 1995)".

In order to verify these stipulations a MINTEQ geochemical computer model simulation was used. Unfortunately, the pH levels of the model depended strongly on the assumptions of the minerals and aqueous compounds present. The model could have increase or decrease in pH using a variety of valid mineral and chemical assemblages. Therefore, without further knowledge of more exacting mineralogical or aqueous chemistry of the site, it is simply speculation at this point that the increase in pH is caused by the oil-field brine exposure.

The importance of pH also has implications on remediation attempts. Several methods for reducing the dispersion hazard of soil have been used in the past. The basic goal is to decrease the sodium adsorption ratio of the soil and increase electrical conductivity. Several minerals applied to soil to accomplish this are gypsum

($CaSO_4H_2O$), calcite ($CaCO_3$) and lime (CaCO). These minerals dissolve in water and increase the relative calcium content of the soil water, which in turn decreased SAR. It also elevates electrical conductivity. The research presented here brings up an important factor that should be considered: a change in pH can increase dispersion in soil. Application of a mineral such as gypsum to a soil can lower pH, and application of calcite can raise pH. Knowing that pH is an important contribution to dispersion, selecting the proper mineral is vital. For example the application of calcite to the soil in this study would increase soil pH. If the gain in electrical conductivity and reduction in SAR are relatively small, the increase in pH will not result in a reduction of dispersion but may in fact increase. This is not a desirable result for the remediation party.

Conclusions

From this research several relevant results, contributions and further questions, beyond the scope of this thesis or research, have come forth. Statistical and neural network analysis on these affected soil indicates a high likelihood that this increase in SAR has caused dispersion. This indicates that sodium is an important contribution to humid-land soil dispersion. Secondly, it was found that an increase in pH is also a contributing factor to dispersion in soil with variably charged minerals. An increase in the pH of the soil may be linked to the same oil-field brine contamination, but is unsubstantiated at this time. This raises the need for further work on the relationship between oil-field brine contamination and pH on this soil. It should be noted that for the applications of minerals such as gypsum or calcite that the potential for changing soil

pH should be considered. A change in pH can cause dispersion, and the intended reduction in dispersion can be negated or further exasperated. Also, based on chemical theory of colloidal forces it has become apparent that linear statistical analysis is inappropriate for the analysis of colloidal dispersion, especially in soil with pH sensitive surface charges. As an alternative non-linear analysis tool neural networks trained using the back-propagation algorithm are useful for analysis of colloid behavior.

CHAPTER V

SPATIAL CORRELATION BETWEEN DISPERSION AND SINKHOLE LOCATIONS

Introduction

The soil data and chemical analysis in this study strongly suggest that dispersion is most likely the initiating mechanism of the sinkholes at the study site. During the initial site investigation it was noted that the E-horizon had experienced the greatest loss by volume and, this layer had a significant loss of colloidal size particles. Plus, the neural network analysis showed the impact on dispersion from increased SAR and pH is strongest in this particular zone. The coincidence of the soil loss in this layer and its dispersion sensitivity is interpreted as evidence that colloidal dispersion from a contaminant that increased SAR and pH lead to a process of soil loss and sinkhole development.

The leading hypothesis for the process of sinkhole development is piping erosion. More specifically, the loss of cohesion within the soil mass from dispersion allowed for the subsurface transport of the soil by some process of piping. Transported soil mass could be removed from the subsurface through some exit point or transported into voids. These pipes could then collapse creating the sinkholes seen at the surface. The difficulty for this hypothesis is finding direct evidence for piping because it is a subsurface process. Providing direct evidence, that the dispersion of the soil is causing piping and sinkhole development, is problematic given the limited knowledge of soil erosion in these dispersible soil and the limited coverage area of tested samples. There

has been evidence that the dispersion of the soil at the site has increased, but the extent to which the increased dispersion has contributed to actual piping erosion is not clear. The exact threshold of increased dispersion that is required to cause subsurface erosion is not certain. One method that could corroborate the relationship of increased dispersion and the piping is spatial correlation. If piping is the process behind the formation of the sinkholes, then a spatial correlation between areas of sinkholes in the areas of increased dispersion should exist. It should be noted that this assumes piping cannot take place in the absence of dispersion in this setting, and that another sinkhole development process that is initiated by dispersion has not occurred.

An approach to linking the increased dispersion to sinkholes is to use the trained neural network and apply it to the geophysical data of apparent conductivity to project a dispersion prediction map that could be compared to the locations of sinkholes. This idea became feasible after the observation that the samples with sodium adsorption ratios greater than the expected background levels have relatively equivalent sodium to calcium plus magnesium ratios. Thus, assuming that this observation can be extrapolated to the geophysical survey area, it is possible to make a prediction of SAR based on the electrical conductivity of the soil. There were three steps necessary to make such a dispersion prediction map: 1) the calibration of electromagnetic induction data to the laboratory electrical conductivity data, 2) the generation of predicted SAR values from that calibrated EC data, and 3) the assumption of the pH levels.

Methods and Results

The geophysical data from the EM-31 is a measurement of electrical conductivity based on a bulk measurement. Its response comes from the top 6 meters of the soil with the peak response situated at 3 meters depth. So, to calibrate the apparent EC data to the laboratory EC data a series of laboratory EC data from various depths of a borehole were averaged and then compared to apparent EC for that same spot. Figure 17 shows the resulting calibration line.

(Note the lack of data distribution)

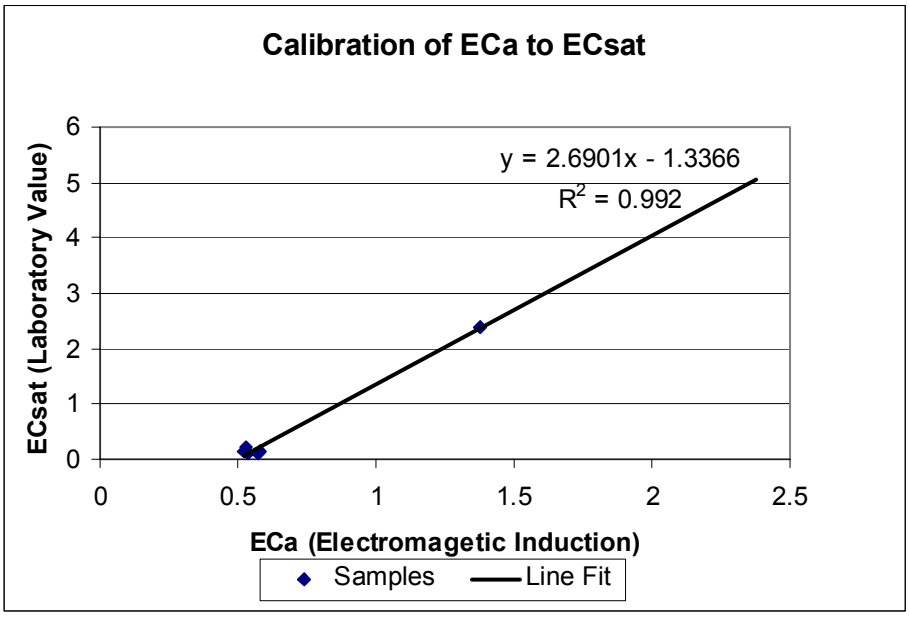

Figure 17. Calibration curve of EC apparent (ECa) to EC saturated paste (ECsat).

It was noted that the average value of the ratio of $Na^{+}/(Ca^{2+}+Mg^{2+})$ is 7.3 (88% of the sum of cations) with a standard deviation of plus or minus 2.825 in samples with a SAR value greater than background levels. This ratio of ions is interpreted to mean that

samples with SAR values greater than three have been contaminated. Using this observation that the ratio of $Na^{+}/(Ca^{2+}+Mg^{2+})$ is relatively similar in samples with a SAR value above background levels, it is possible to predict SAR from the calibrated EC data. This is because the EC of the saturated paste is directly proportional to the sum of cations ($Na^{+}+Ca^{2+}+Mg^{2+}+K^{+}$) in solution (Figure 18).

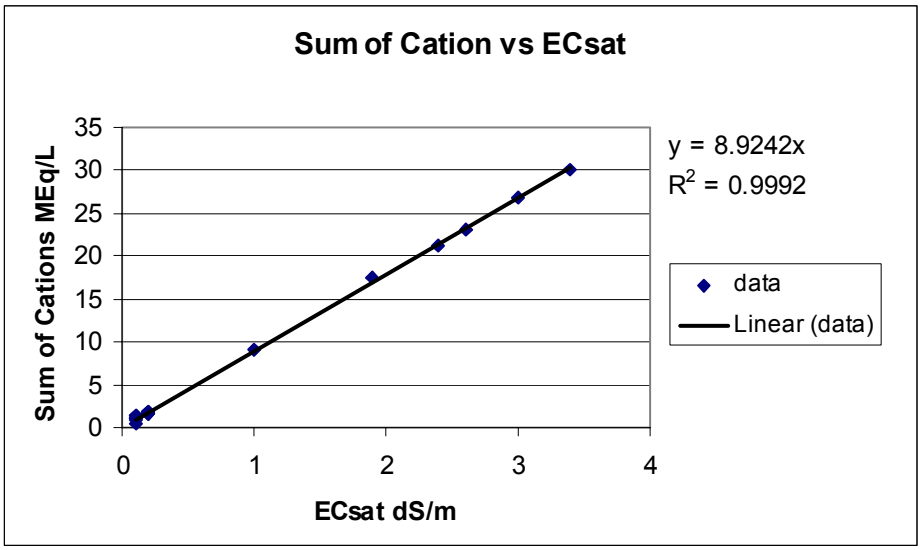

Figure 18. Calibration curve for sum of cations from EC saturated paste.

With EC known the sum of cations can be very reliably calculated. Thus, from the EC measurements a prediction of SAR can be made using the following equation.

$$SAR_p = \frac{8.9(EC)0.88}{\sqrt{(8.9(EC)0.12)/2}}$$

The predicted SAR levels are compared to actual EC levels in Figure 19.

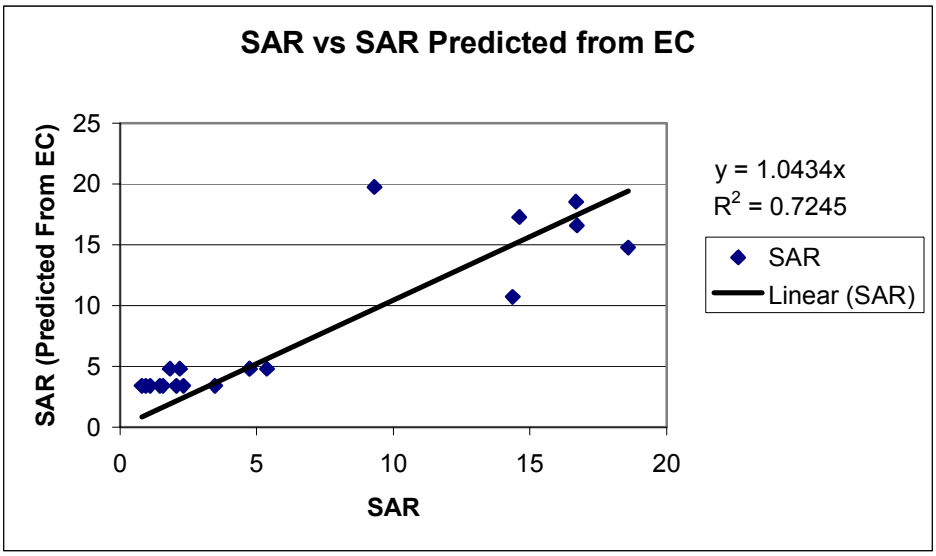

Figure 19. Fit of predicted SAR to actual SAR.

The predictive model for dispersion also needed pH as an input parameter. However, it is not possible to infer pH by the remote sensing techniques available. Therefore an average pH value of 6.5 was selected. Also, a depth variable is needed for the predictive model of dispersion. Given the knowledge that soil variegate into horizons of similar mineralogy and organic content with depth, the depth parameter serves as a qualitative variable for soil mineralogy and organic content that is important to colloid behavior. It was found that a depth of 55cm was very sensitive to dispersion during the data analysis. This depth also corresponded to the interval of greatest soil volume loss and colloid loss by mass. Given these two factors, it was decided that a depth of 55cm should be used for the predictive model.

The predictive model selected is the neural network trained with laboratory data (Chapter IV). The input parameters of calibrated EC, projected SAR, depth variable of 55 cm and a pH of 6.5 were run through the neural network to generate a dispersion output. This data was then interpolated to create a map of predicted dispersion on which the locations of sinkholes were placed for the spatial correlation between dispersion and sinkhole development (Figure 20). Data that were clearly affected by surface debris were removed from the data set for constructing the prediction map. This was done to insure that only the ground response was considered. The resulting map shows some relationship between increased potential for dispersion and the location of sinkholes.

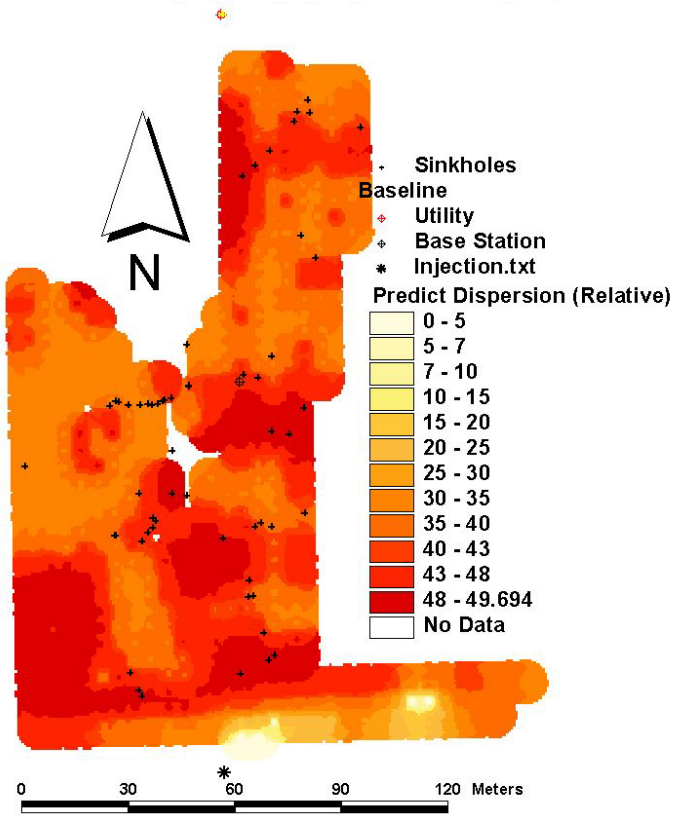

Figure 20. Map of predicted relative-dispersion with sinkhole locations.

Discussion

Most of the sinkholes lie within areas with predicted a relative-dispersion value greater than 40. This indicates a correlation between increased dispersion and the appearance of sinkholes. This result would be expected for a process such as piping erosion, where increased dispersion would increase piping and sinkholes. However, in some areas with the highest predicted relative-dispersion levels there are no sinkholes.

The primary example of this is the southwest region of the study area with predicted relative-dispersion values in excess of 48. This particular area is different from the rest of the high dispersion potential areas, because it lacks tree or shrub cover that is found in the other affected areas. This may imply that the process of the sinkhole formation needs the cohesion supplied by extensive root systems to support soil pipes. Given the knowledge that the area soils have low cohesion, a soil pipe may not be possible without some sort of cohesive framework to support the pipe structures for the transport of sediment without collapse. Thus, dispersion may be taking place in these open areas without resulting in piping because it lacks the needed cohesive framework.

Aside from the observation that some of the areas of high potential dispersion lack sinkholes, there is also the problem of sinkholes occurring in areas of marginal predicted dispersion. Many of these sinkholes are found in the area where surface interference or poor data density may be a problem. The central section of the map with no data resulted from the removal of conductivity data clearly affected by surface interference. It is also possible that these areas have pH levels higher than the assumed 6.5, which would increase the dispersion potential despite moderate SAR levels. Also,

this map relies on current data. In the past the conditions for dispersion may have been higher in the area where these sinkholes currently exist.

Uncertainty Within the Model

The dispersion predictive map shows a correlation between predicted dispersion and the location of the sinkholes. However, there are considerable levels of uncertainty in this map because of assumptions made during in the construction of the dispersion prediction model.

The foremost source of uncertainty is the value of the geophysical techniques for measuring soil-water electrical conductivity. The apparent electrical conductivity measurement from frequency domain electromagnetics is dependant upon the fluid content, fluid chemistry, texture, and mineralogy of the soil. This predictive model is based on the assumption that apparent conductivity is a measure of soil water EC. Thus, the other parameters of texture, mineralogy and fluid content are assumed to be homogenous throughout the coverage area. Given the depth of the response to the EM-31, and the observations of homogeneity with depth from cores, that assumption is probably close. However, there are enough variations in surface topography and vegetation to question just how reliable that assumption is. Compounding this problem is the lack of distribution in the calibration measurements. The calibration curve is heavily influence by the samples taken from within the high conductivity area, which contributes to statistical uncertainty.

The second most important source of uncertainty is the predictive model for SAR from EC. The logic behind using the observation that the ratio of $Na^{+}/(Ca^{2+}+Mg^{2+})$ is relative constant for predicting SAR from EC measurements is based on the interpretation that the samples were all affected by a contaminant of similar ion content. This interpretation may be valid for the sampled area, but when applying this interpretation to other parts of the study area it is questionable whether the same contaminant is to blame for increased apparent conductivity readings. Even within the data, on which this interpretation was made, there are significant amounts of variation. The affect of this variation is illustrated in figure 19 (page 83); the fit of the predicted SAR levels has a marginal fit to the actual SAR values.

The final problem is the use of a single pH value for the entire study area. The analysis of the chemical data for the relationship to dispersion showed a strong dependence on pH. The chemical analysis found wide variations in pH, ranging from pH 4.8 to 7.2. The pH may vary across the study area depending on contaminant levels and biologic activity. Given the importance of pH on dispersion and the potential for variation, using a single value of pH results in a significant contribution to uncertainty of the model. The uncertainty of the EC, SAR and pH values used in the predictive model weaken the value of this prediction of dispersion and the implications on sinkhole development.

Alternative Study Method

A direct sampling grid covering the entire study area would supply data that would be immune from the uncertainty problems implicated in using geophysical data. Direct sampling of the study area would produce reliable numbers for SAR, EC and pH. This data could then be used in the predictive model to give prediction of dispersion for the sample locations. A geostatistical method such as kriging or simple interpolation could then be used to make a map from the data for correlation studies to sinkhole locations. The sampling and analysis could be streamlined for the specific depth of interest. The drawback to this method is economic limitations; an exhaustive sampling and analysis program can be costly. In cases of limited funding a sampling and analysis program used in conjunction with highly calibrated geophysical data could yield the desired spatial resolution and certainty levels, and yet control costs.

Conclusions

The predicted dispersion has a spatial correlation to the location of sinkholes on the study site. This implies that dispersion is the mechanism responsible for the formation of the sinkholes, most likely through the process of piping erosion. This predictive model has significant levels of uncertainty because of several assumptions. A more conclusive study would require extensive direct sampling.

CHAPTER VI

SUMMARY AND CONCLUSIONS

The hypothesis that a sodium contaminant caused dispersion of the soil at the site and allowed for the development of sinkholes is supported by the conclusions of extensive research. It should be noted that a degree of uncertainty remains because of a lack of data coverage and calibration data. With appropriate funding, further research beyond the scope of this thesis can remove much of the reasonable uncertainty.

From studying the existing literature of similar occurrences and the morphology and distribution of the sinkholes, piping erosion appeared to be the most likely process. From observations of the landscape and soil at the study site it became apparent that a localized and recent environmental-pressure, probably an anthropogenic change, was the most likely triggering event for the sinkhole development process. Thus, the research objective was to find the environmental pressure that caused the piping or similar process to occur.

The site investigation led to the discovery of several anomalous characteristics of the site, which helped explain the process by which the sinkholes are forming. The geophysical investigation of the site led to the important discovery that the high apparent conductivity zone, most probably from a release of brine from the nearby injection well, coincided with the observation of sinkholes. Also, from the hydrologic investigation it was found that the saturated hydraulic conductivity was 10 to 50 times greater in the sinkholes, which supports the idea that the sinkholes are related to a hydraulic conduit such as piping. Plus, by comparing and contrasting a set of cores within and outside of a

sinkhole it was found that the core of the sinkhole soil is depleted in colloid size particles in the E-horizon, which appears to be the primary horizon for volume loss.

The loss of the colloids has strong implications. Soil colloids, usually clay minerals, have strong cohesive forces, which bind soil together making it difficult to entrain by fluids. The break down in cohesion of the soil, also known as dispersion, could allow for the depletion of the colloids through piping. There are several triggers of dispersion including the addition of sodium to colloid surfaces. Soil analysis indicated that some areas of the site have elevated levels of sodium thought to be sufficient for dispersion.

Given the hydrologic conditions at the site it is possible that the area of the sinkholes may have been exposed to sodium by a release of brine from a nearby injection well. Brine contamination fits with the idea that the pressure on the landscape is a recent and most likely anthropogenic event. Brine contamination also explains the localized nature of the sinkholes in an otherwise similar landscape. However, because of reasonable doubt and lack of precedent that high sodium levels could contribute to dispersion in this particular setting, further research into the affect of sodium on dispersion for this case was undertaken.

Soil samples from the study site were analyzed for parameters pertinent to colloid dispersion including: sodium adsorption ratios, electrical conductivity and pH. Both the statistical and neural network analysis indicated that increased levels of sodium adsorption ratios lead to greater levels of dispersion. This provides the strongest evidence yet for sodium-induced dispersion at this study site.

During the initial site investigation it was noted that the E-horizon has a significant loss of colloidal size particles. From the neural network analysis the impact on dispersion from increased SAR and pH is strongest on this particular zone. The coincidence of the soil loss of this layer and its dispersion sensitivity is interpreted as evidence that colloidal dispersion from a contaminant, that increased SAR and pH, lead to the soil loss and sinkhole development

Finally, an attempt to use the trained neural network and apparent conductivity data to predict dispersion showed spatial correlation between the observation of sinkholes and predicted dispersion. Although this attempt suffers from lack of calibration data and inherent non-uniqueness, it adds to the idea that the dispersion of soil colloids is causing sinkholes to develop. It also acts as a framework from which future work may be based for the prediction of sodium-induced dispersion.

Contributions

Aside from finding a mechanism that can explain the appearance of the sinkholes this research has resulted in several contributions for the analysis and prediction of colloidal dispersion in natural systems. This research showed that sodium is an important factor in the dispersion of colloids in humid soil. Sodium induced dispersion is popularly thought to only affect arid to semiarid soil with high CEC and expansive clays (e.g. Jones, 1990). This study also shows the effectiveness of neural networks for nonlinear analysis of dispersion in cases of incomplete or noisy data. It also shows promise of calibrated EM data and neural networks for the prediction of piping.

REFERENCES

Aitchison, G.D., and Wood, C.C., 1965, Some interactions of compaction, permeability, and post-construction deflocculation affecting the probability of piping failure in small earth dams, in *Proceedings of the 6th International Conference on Soil Mechanics and Foundation Engineering*, Montreal, 2, pp. 442-446.

Aldridge, C., 2001, Personal Communication, Site Landowner, Cleveland, TX.

Bair, E.S., and Digel, R.K., 1990, Subsurface transport of inorganic and organic solutes from experimental road spreading of oil-field brine: *Ground Water Monitoring Review*, Vol. 10, pp. 94-105.

Barrett, M.L., 2002, Saltwater waste and landscape change, Smackover Field, Arkansas: *Environmental Geosciences*, Vol. 9, pp. 17-28.

Bazin, B., Brosse, E., and Sommer, F., 1997, Chemistry of oil-field brines in relation to diagenesis of reservoirs 1. Use of mineral stability fields to reconstruct in situ water composition. Example of the Mahakam basin: *Marine and Petroleum Geology*, Vol. 14, pp. 481-495.

Benard, H. A., LeBlanc, R. J., and Major, C. F., 1962, Recent and Pleistocene geology of Southeast Texas. In Rainwater, E. H. and Zingula, R. P. (Editors), *Geology of the Gulf Coast and Central Texas, and Guidebook of Excursions*, Houston Geological Society for the 1962 annual meeting of the Geological Society of America and Associated Societies, Houston, TX., Field Excursion No. 3, pp. 175-224.

Berger, Z., and Aghassy, J., 1984, Near-surface groundwater and evolution of structurally controlled streams in soft sediments. In LaFleur, R.G. (Editor), *Groundwater as a Geomorphic Agent*, Allen and Unwin, Boston, pp.59-77.

Bloom, A. L., 1998, *Geomorphology: A Systematic Analysis of Late Cenozoic Landforms*, *3rd edition*: Prentice Hall, Upper Saddle River, NJ, 482 p.

Bowen, D. Q., 1978, *Quaternary Geology; A Stratigraphic Framework for Multidisciplinary Work*: Pergamon Press, Oxford, 221 p.

Bresler, E., McNeal, B. L., and Cater, D. L., 1982, *Saline and Sodic Soil: Priciples-Dynamics-Modeling*: Springer-Verlag, New York, 236 p.

Cedergren, H. R., 1977, *Seepage, Drainage, and Flow Nets, 2nd edition*: John Wiley and Sons, New York, 534 p.

Das, B.M., 2000, *Fundamentals of Geotechnical Engineering*: Brooks/Cole, Pacific Grove, CA, 593 p.

Domenico, P.A., and Schwartz, F.W., 1998, *Physical and Chemical Hydrogeology, 2nd edition*: John Wiley & Sons, New York, 506 p.

Durgin, P.B., 1984, Subsurface drainage erodes forested granitic terrane: *Physical Geography*, Vol. 4, pp. 24-39.

Durgin, P. B., and Chaney, J. G., 1984, Dispersion of kaolinite by dissolved organic matter from Douglas-Fir roots: *Canadian Journal of Soil Science*, Vol. 64, pp. 445-455.

Everett, M., 2002, Personal Communication, Professor of Geophysics, Texas A&M University, College Station.

Faulkner, H., Spivey, D., and Alexander, R., 2000, The role of some site geochemical processes in the development and stabilization of three badland sites in Almeria, Southern Spain: *Geomorphology*, Vol. 35, pp. 87-99.

Fetter, C.W., 1999, *Contaminant Hydrogeology, 2nd edition*: Prentice Hall, Upper Saddle River, NJ, 500 p.

Foss, J.E., and Segovia, A.V., 1984, Rates of soil formation. In LaFleur, R.G. (Editor), *Groundwater as a Geomorphic Agent*, Allen and Unwin, Boston, pp. 19-58.

Freed, L.S., Savage, C., and Howarth, L., 1996, A Pleistocene-Holocene soil profile in the lower Lissie (Bentley) Formation. In Cooper, R. W., Stevens, J. B., Owen, D. E., and Westgate, J. W. (Editors), *Transect of the Upper Texas Gulf Coast: Geology, Resources, Environment*: Southwestern Association of Student Geologic Societies, Beaumont, TX, pp. 56-63.

Griffith, K. L., Holland, P. D., and Feurerbacher, T. A., 1996, *Soil Survey of Liberty County, Texas*: United States Department of Agriculture, Natural Resources Conservation Service, in cooperation with Texas Agricultural Experiment Station and Texas State Soil and Water Conservation Board., Washington D.C., vii, 192 p., [3], 61 folded leaves of plates : ill., maps; 28 cm.

Güven, N., 1992, Molecular aspects of clay-water interactions. In Güven, N., and Pollastro, R.M. (Editors), *Clay-Water Interactions and Its Rheological Implications*: CMS Workshop Lectures, Vol. 4, Aurora, CO, pp. 1-80.

Hallmark, C., 2003, Personal Communication, Professor of Soil and Crop Science, Texas A&M University, College Station.

Herbert, B., 2002, Personal Communication, Professor of Geology, Texas A&M University, College Station.

Higgins, C. G., 1984, Piping and sapping: Development of landforms by groundwater outflow. In LaFleur, R.G. (Editor), *Groundwater as a Geomorphic Agent*: Allen and Unwin, Boston, pp. 19-58.

Higgins, C. G., and Schoner, C., 1997, Sinkholes formed by piping into buried channels: *Geomorphology*, Vol. 20, pp. 307-312.

Holtzer, T. L., 1984, *Man-induced Land Subsidence: Review of Engineering Geology VI*: Geologic Society of America, Boulder, CO, 221 p.

Hunter, D., Isphording, W. C., and Flowers, G. C., 1989, Karst development in coastal plains sands; a "new" problem in foundation engineering; discussion and reply: *Bulletin of the Association of Engineering Geologists*, 26; Vol. 3, pp. 397-401.

Isphording, W. C.,and Flowers, G. C., 1988, Karst development in coastal plains sands; a "new" problem in foundation engineering: *Bulletin of the Association of Engineering Geologists*, Vol. 25, pp. 95-104.

Jones, J.A.A., 1990, Piping effects in humid lands. In Higgins, C. G., and Coates, D. R. (Editors), *Groundwater Geomorphology: The Role of Subsurface Water in Earth-Surface Processes and Landforms*: G.S.A special paper 252, pp. 111-138.

Langmuir, D., 1997, *Aqueous Environmental Geochemistry*, Prentice Hall, Upper Saddle River, New Jersey, 600 p.

Little, I. P., 1989, A dispersibility index for soil and its dependence on other soil properties tested with a group of soil from the Lockyer Valley Uplands, Qld., and the lower Namoi Valley, N. S. W.: *Australian Journal of Soil Research*, Vol. 27, pp. 493-509.

McNeill, J.D., 1980, *Technical Note TN-6: Electromagnetic Terrain Conductivity Measurement at Low Induction Numbers*: Geonics Limited, Ontario, Canada, 15 p.

Minhas, P. S., Singh, Y. P., Chhabba, D. S., and Sharma, V. K., 1999, Changes in hydraulic conductivity of soil varying in calcite content under cycles of irrigation with saline-sodic and simulated rain water: *Irrigation Science*, Vol. 18, pp. 199-203.

Olphen, H. van, 1991, *Clay Colloid Chemistry for Clay Technologists, Geologists, and Soil Scientists*, *2nd edition*: Krieger Publishing, Malabar, FL, 318 p.

Ooyen, A. V., and Nienhuis, B., 1992, Improving the convergence of the back-propagation algorithm: *Neural Networks*, Vol. 5, pp. 465-471.

Ott, R.L., and Longnecker, M., 2001, *An Introduction to Statistical Methods and Data Analysis*, *5th edition*: Duxbury, Pacific Grove, CA, 1152 p.

Parker, G.G., Higgins, C. G, and Wood, W. W., 1990, Piping and psuedokarst in drylands. In Higgins, C. G., and Coates, D. R. (Editors), *Groundwater Geomorphology: The Role of Subsurface Water in Earth-Surface Processes and Landforms*: G.S.A special paper 252,Boulder, CO, pp. 77-110.

Pewe, T. L., 1990, Land subsidence and earth-fissure formation caused by groundwater withdrawal in Arizona; A review. In Higgins, C. G., and Coates, D. R. (Editors), *Groundwater Geomorphology*: *The Role of Subsurface Water in Earth-Surface Processes and Landforms*: G.S.A special paper 252, Boulder, CO, pp. 219-233.

Rengasamy, P., Greene, R.S.B., Ford, G.W., and Mehanni, A.H., 1984, Identification of dispersive behaviour and the management of red-brown earths: *Australian Journal of Soil Research*, Vol. 22, pp. 413-431.

Rumelhart, D. E., Hinton, G. E.,and Williams, R. J., 1986, Learning representations by back-propagating errors: *Nature*, Vol. 323, pp. 533-536.

Seaman, J.C., Bertsch, P.M., and Strom, R.N., 1997, Characterization of colloids mobilized from southeastern coastal plain sediments: *Environmental Science and Technology*, Vol. 31, pp. 2782-2790.

Shainberg, I., Rhoades, J. D., and Prather, R. J., 1980, Effect of low electrolyte concentration on clay dispersion and hydraulic conductivity of a sodic soil: *Soil Science Society of America Journal*, Vol. 45, pp. 273-277.

Sharma, P. V., 1997, *Environmental and Engineering Geophysics*: Cambridge University Press, Cambridge, UK, 475 p.

Soil Survey Staff, 2003, *National Soil Survey Characterization Data*: Soil Survey Laboratory National Soil Survey Center USDA-NRCS, Lincoln, NE, Available online: http://soils.usda.gov/.

Steeb, W.H., 1999, *The Nonlinear Workbook*: World Scientific Publishing, River Edge, NJ, 585 p.

Tamayo, 2001, Personal Communication, Site Landowner, Cleveland, TX.

Whittemore, D.O., 1995, Geochemical differentiation of oil-field and gas brine from other saltwater sources contaminating water resources: Case studies from Kansas and Oklahoma: *Environmental Geosciences*, Vol. 2, pp. 15-31.

Williams, M., Dunkerley, D., Deckker, P.D., Kershaw, P.,and Chappell, J., 1998, *Quaternary Environments, 2nd edition*: Oxford University Press Inc., New York, 329 p.

Yariv, S., and Cross, H., 1979, *Geochemistry of Colloid Systems for Earth Scientists*: Springer-Verlag, New York, 450 p.

VITA

Douglas Spencer Sassen

Permanent Address:

16017 Woodlake Dr.

College Station, TX 77845

Douglas earned his Bachelor of Science in geology from the University of Texas at Austin in August 2000. He worked as an undergraduate assistant in the Sedimentary Core Laboratory at the University of Texas Geology Department from 1998 to 2000. From May 2000 until December 2000 Douglas worked as a research assistant at the Bureau of Economic Geology in Austin, Texas as a programmer and GIS technician. He came to Texas A&M University in January 2001 to work on a Master of Science in geology and to work as a graduate teaching assistant. Douglas received his Master of Science in December 2003.